# An Inverse Source Technique for the Design of Reflectarrays with Constrained Phase Distributions

**M. Salucci, G. Oliveri, and A. Massa**

# Contents

Part I

# Numerical Analysis

# 1 Phase Range [-135:135] - Test Case 1 - 55x55 - Linear Polarization

## 1.1 K=400, P=10, I=100000

In the Fig. 1 is depicted the behaviour of the Cost Function varying the random seed. The best value of cost function is achieved by Seed=2 and is $\Phi = 4.263 \times 10^{-1}$.

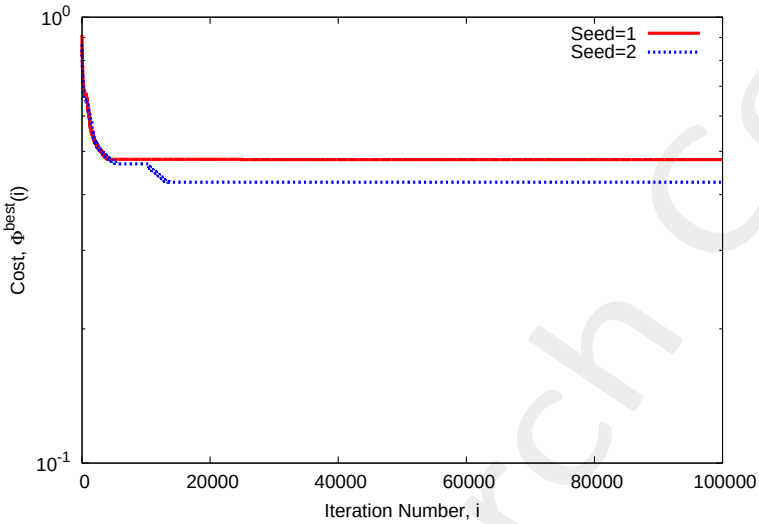


Figure 1: Cost Function behaviour at different random seed.

At this value of cost function the achieved performance on the Phase are showed in Fig. 2 and are numerically showed in table I.

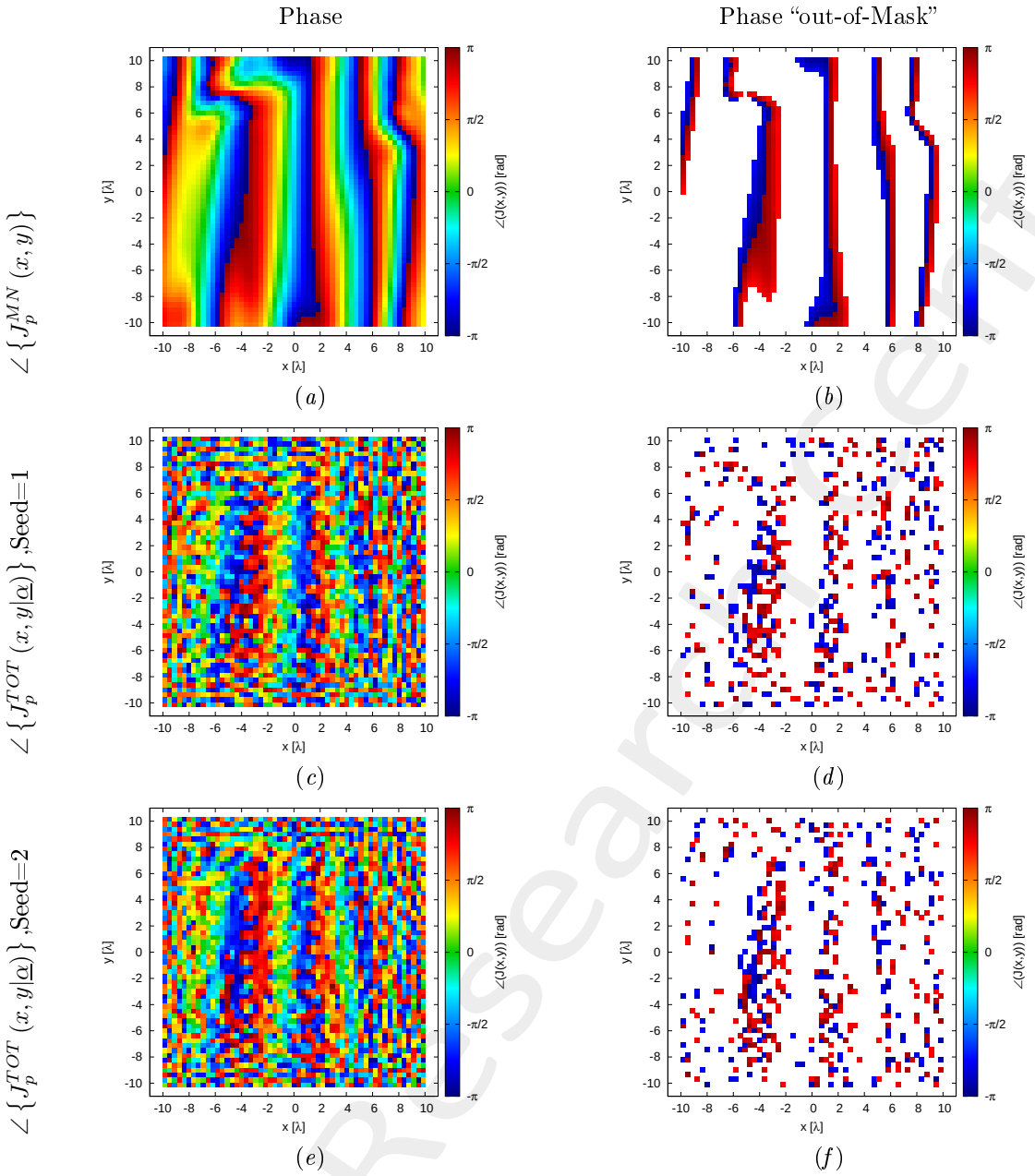


Figure 2: Phase $(a)(c)(e)$ and value of the phase out of the minimization range $(b)(d)(f)$ of the Minimum-Norm current $(\angle\{J_p^{MN}(x,y)\})(a)(b)$, of the total current for the random seed $= 1(c)(d)$ and for the random seed $= 2(e)(f)$.

| Case | Φ | Number of value $> \phi_p^{MAX}(x,y)$ | Number of value $< \phi_p^{MIN}(x,y)$ | Phase Range | | Time $[s]$ |
|---|---|---|---|---|---|---|
| | | | | Min $[deg]$ | Max $[deg]$ | |
| $MN$ | 1.0 | 451 | 358 | $-179.87$ | 179.63 | |
| Seed=1 | $4.791 \times 10^{-1}$ | 292 | 248 | $-179.23$ | 179.00 | $1.20 \times 10^4$ |
| Seed=2 | $4.263 \times 10^{-1}$ | 279 | 229 | $-179.89$ | 179.26 | $1.19 \times 10^4$ |

Table I: Cost Function value and statistics about the result.

The verification of the radiated field is showed in Fig. 3 and numerically in table II.

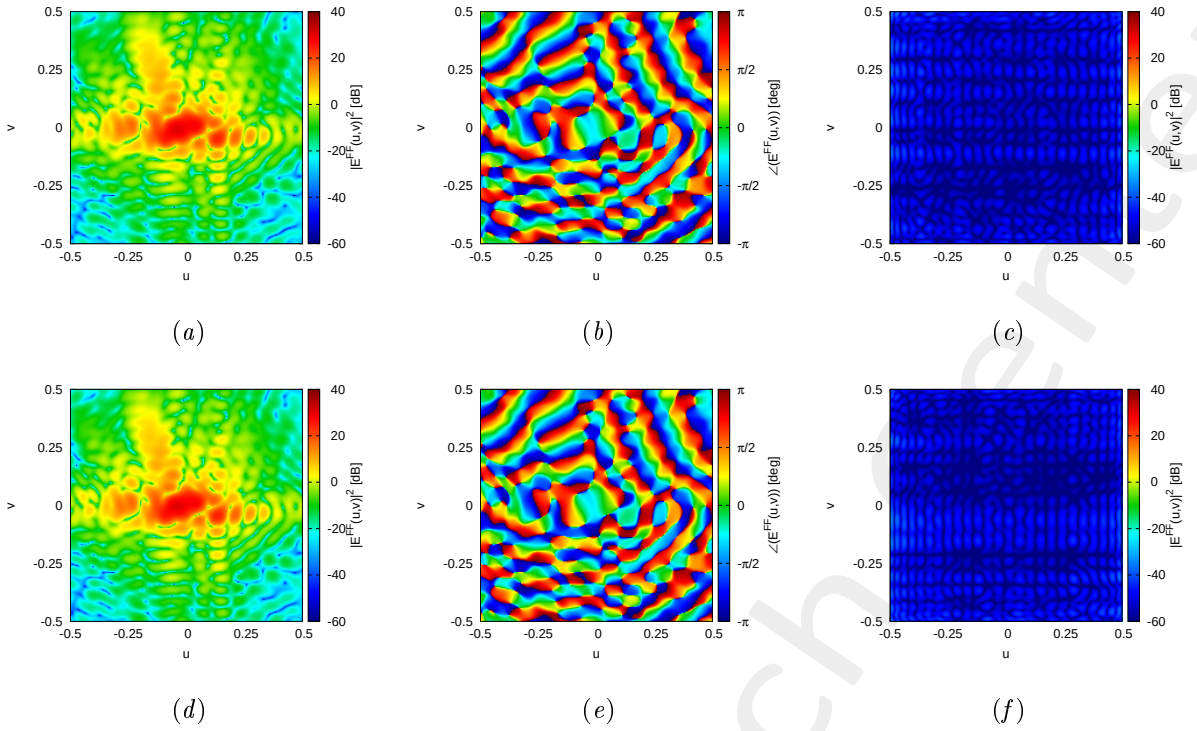


Figure 3: Magnitude $(a)(d)$, Phase $(b)(e)$ and Magnitude of the difference with respect to the original field $(c)(f)$ of the seed=1 $(a)(b)(c)$ and seed=2 $(d)(e)(f)$.

| Seed | $\xi$ |
|---|---|
| 1 | $1.98 \times 10^{-3}$ |
| 2 | $2.05 \times 10^{-3}$ |

Table II: Integral error of the difference between the original field and the one radiated by the total current.

## 1.2 K=400, P=20, I=100000

In the Fig. 4 is depicted the behaviour of the Cost Function varying the random seed. The best value of cost function is achieved by Seed=2 and is $\Phi = 3.445 \times 10^{-1}$.

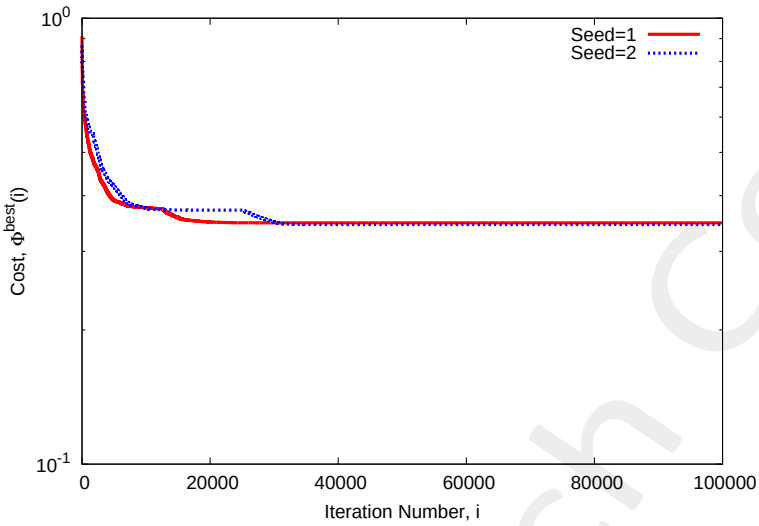


Figure 4: Cost Function behaviour at different random seed.

At this value of cost function the achieved performance on the Phase are showed in Fig. 5 and are numerically showed in table III.

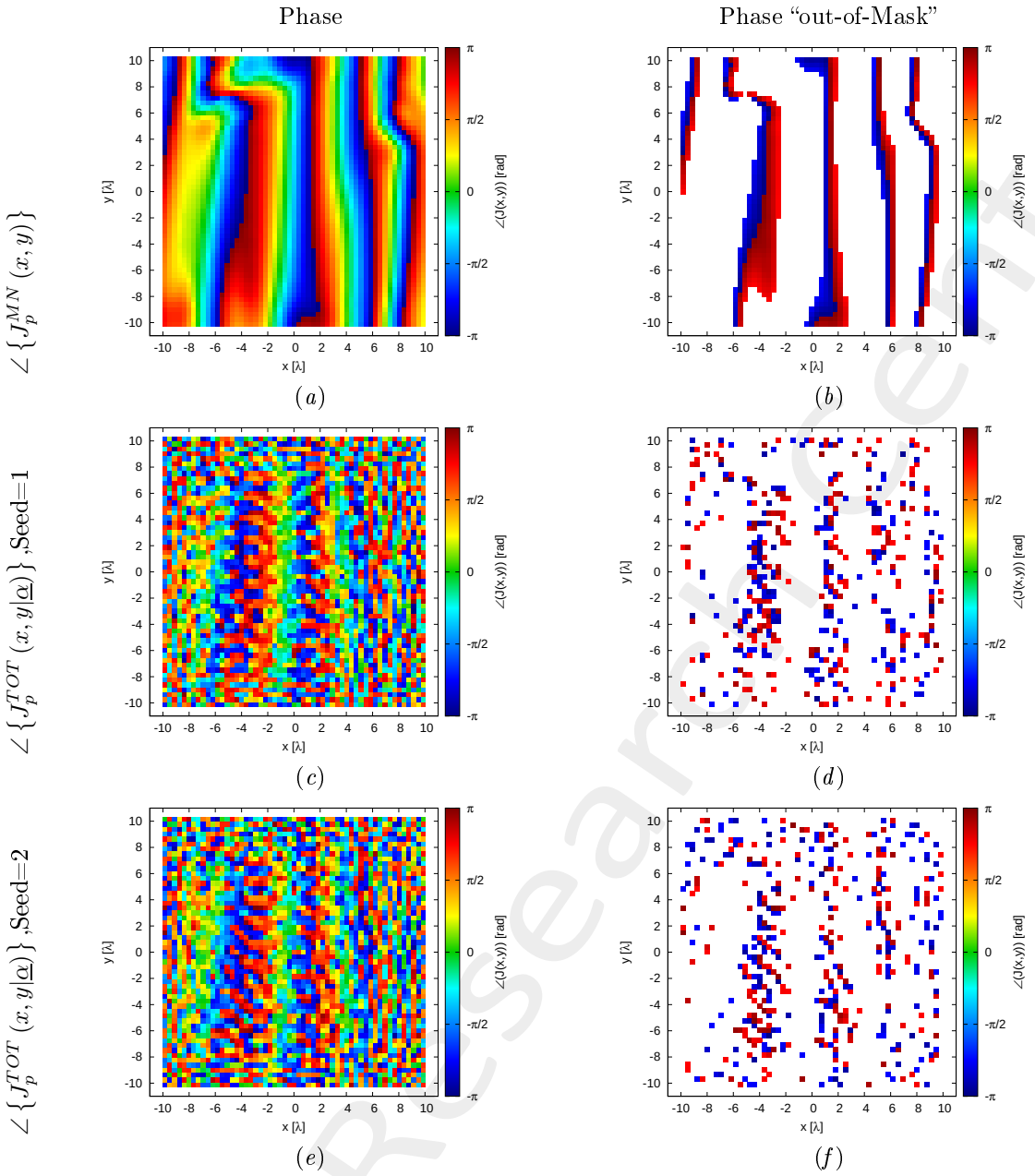


Figure 5: Phase $(a)(c)(e)$ and value of the phase out of the minimization range $(b)(d)(f)$ of the Minimum-Norm current $(\angle\{J_p^{MN}(x,y)\})(a)(b)$, of the total current for the random seed $= 1(c)(d)$ and for the random seed $= 2(e)(f)$.

| Case | Φ | Number of value $> \phi_p^{MAX}(x,y)$ | Number of value $< \phi_p^{MIN}(x,y)$ | Phase Range | | Time $[s]$ |
|---|---|---|---|---|---|---|
| | | | | Min $[deg]$ | Max $[deg]$ | |
| $MN$ | 1.0 | 451 | 358 | $-179.87$ | 179.63 | |
| Seed=1 | $3.476 \times 10^{-1}$ | 234 | 208 | $-179.84$ | 178.75 | $2.44 \times 10^4$ |
| Seed=2 | $3.445 \times 10^{-1}$ | 211 | 220 | $-177.73$ | 179.60 | $2.23 \times 10^4$ |

Table III: Cost Function value and statistics about the result.

The verification of the radiated field is showed in Fig. 6 and numerically in table IV.

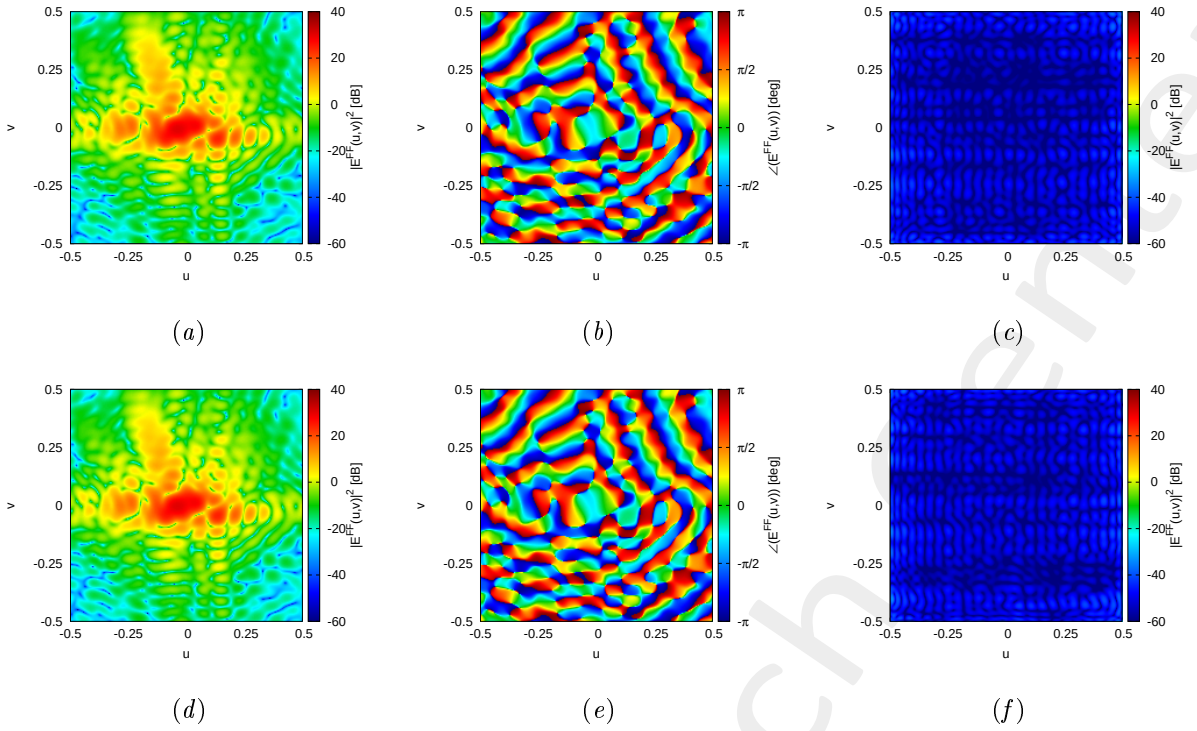


Figure 6: Magnitude $(a)(d)$, Phase $(b)(e)$ and Magnitude of the difference with respect to the original field $(c)(f)$ of the seed=1 $(a)(b)(c)$ and seed=2 $(d)(e)(f)$.

| Seed | $\xi$ |
|---|---|
| 1 | $1.97 \times 10^{-3}$ |
| 2 | $2.14 \times 10^{-3}$ |

Table IV: Integral error of the difference between the original field and the one radiated by the total current.

### 1.3 K=400, P=40, I=100000

In the Fig. 7 is depicted the behaviour of the Cost Function varying the random seed. The best value of cost function is achieved by Seed=1 and is $\Phi = 3.177 \times 10^{-1}$.

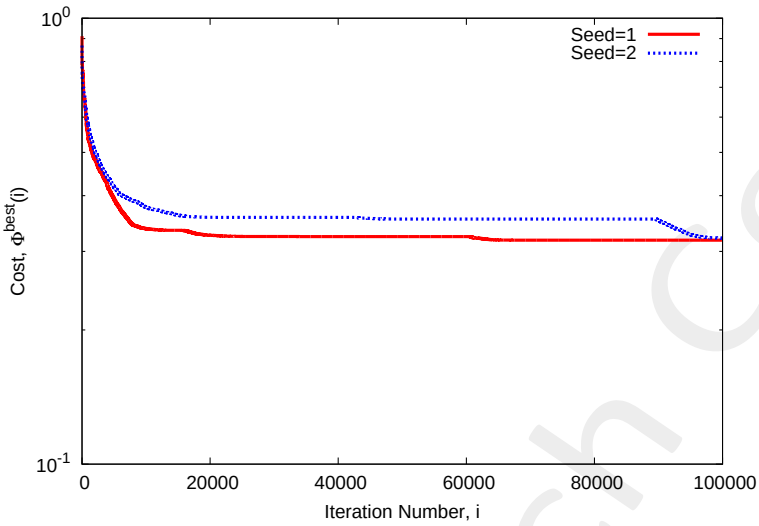


Figure 7: Cost Function behaviour at different random seed.

At this value of cost function the achieved performance on the Phase are showed in Fig. 8 and are numerically showed in table V.

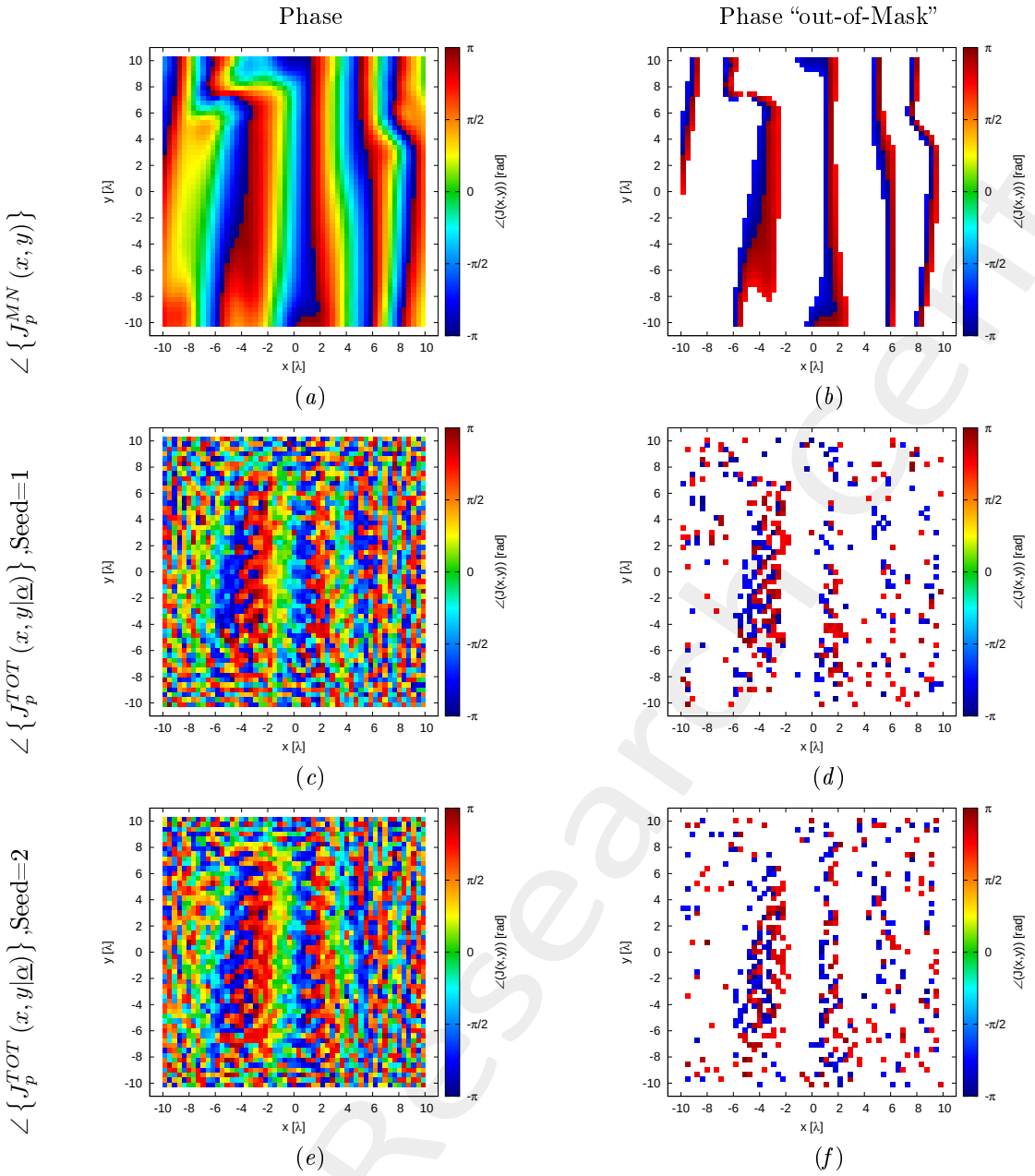


Figure 8: Phase $(a)(c)(e)$ and value of the phase out of the minimization range $(b)(d)(f)$ of the Minimum-Norm current $(\angle\{J_p^{MN}(x,y)\})(a)(b)$, of the total current for the random seed $= 1(c)(d)$ and for the random seed $= 2(e)(f)$.

| Case | Φ | Number of value $> \phi_p^{MAX}(x,y)$ | Number of value $< \phi_p^{MIN}(x,y)$ | Phase Range | | Time $[s]$ |
|---|---|---|---|---|---|---|
| | | | | Min $[deg]$ | Max $[deg]$ | |
| $MN$ | 1.0 | 451 | 358 | $-179.87$ | 179.63 | |
| Seed=1 | $3.177 \times 10^{-1}$ | 224 | 202 | $-179.19$ | 179.82 | $4.56 \times 10^4$ |
| Seed=2 | $3.211 \times 10^{-1}$ | 228 | 202 | $-176.96$ | 178.56 | $4.53 \times 10^4$ |

Table V: Cost Function value and statistics about the result.

The verification of the radiated field is showed in Fig. 9 and numerically in table VI.

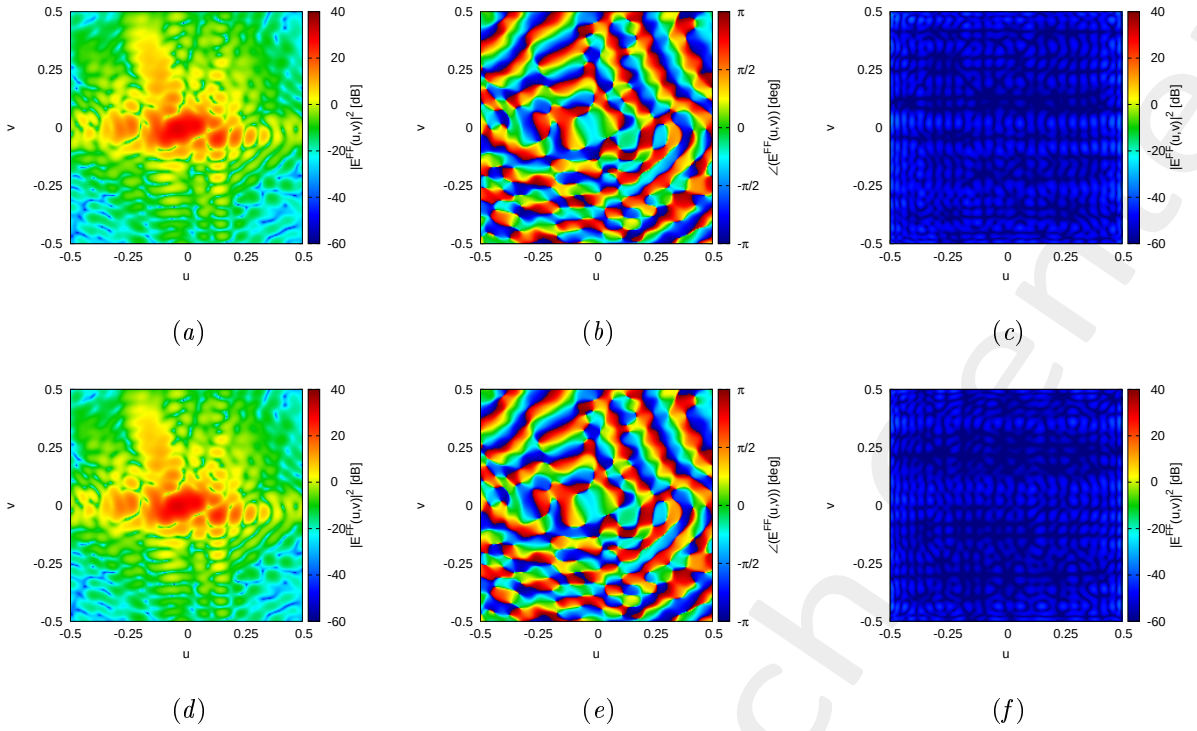


Figure 9: Magnitude $(a)(d)$, Phase $(b)(e)$ and Magnitude of the difference with respect to the original field $(c)(f)$ of the seed=1 $(a)(b)(c)$ and seed=2 $(d)(e)(f)$.

| Seed | $\xi$ |
|---|---|
| 1 | $2.11 \times 10^{-3}$ |
| 2 | $1.81 \times 10^{-3}$ |

Table VI: Integral error of the difference between the original field and the one radiated by the total current.

## 1.4 Observation

The best result is obtained with the combination $K = 200$ and $P = 40$. Hovewer, all the results have a very high variance (at the variation of the random seed) as can be seen, for example, in Fig. 10. Thus, we propose to increase the population for the higher value of $K$.

## 1.5 K=400, P=80, I=300000

In the Fig. 10 is depicted the behaviour of the Cost Function varying the random seed. The best value of cost function is achieved by Seed=1 and is $\Phi = 1.919 \times 10^{-1}$.

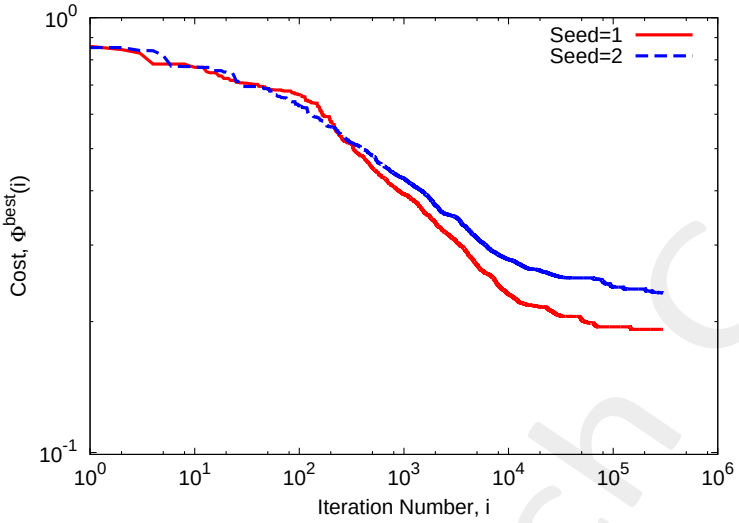


Figure 10: Cost Function behaviour at different random seed.

At this value of cost function the achieved performance on the Phase are showed in Fig. 11 and are numerically showed in table VII.

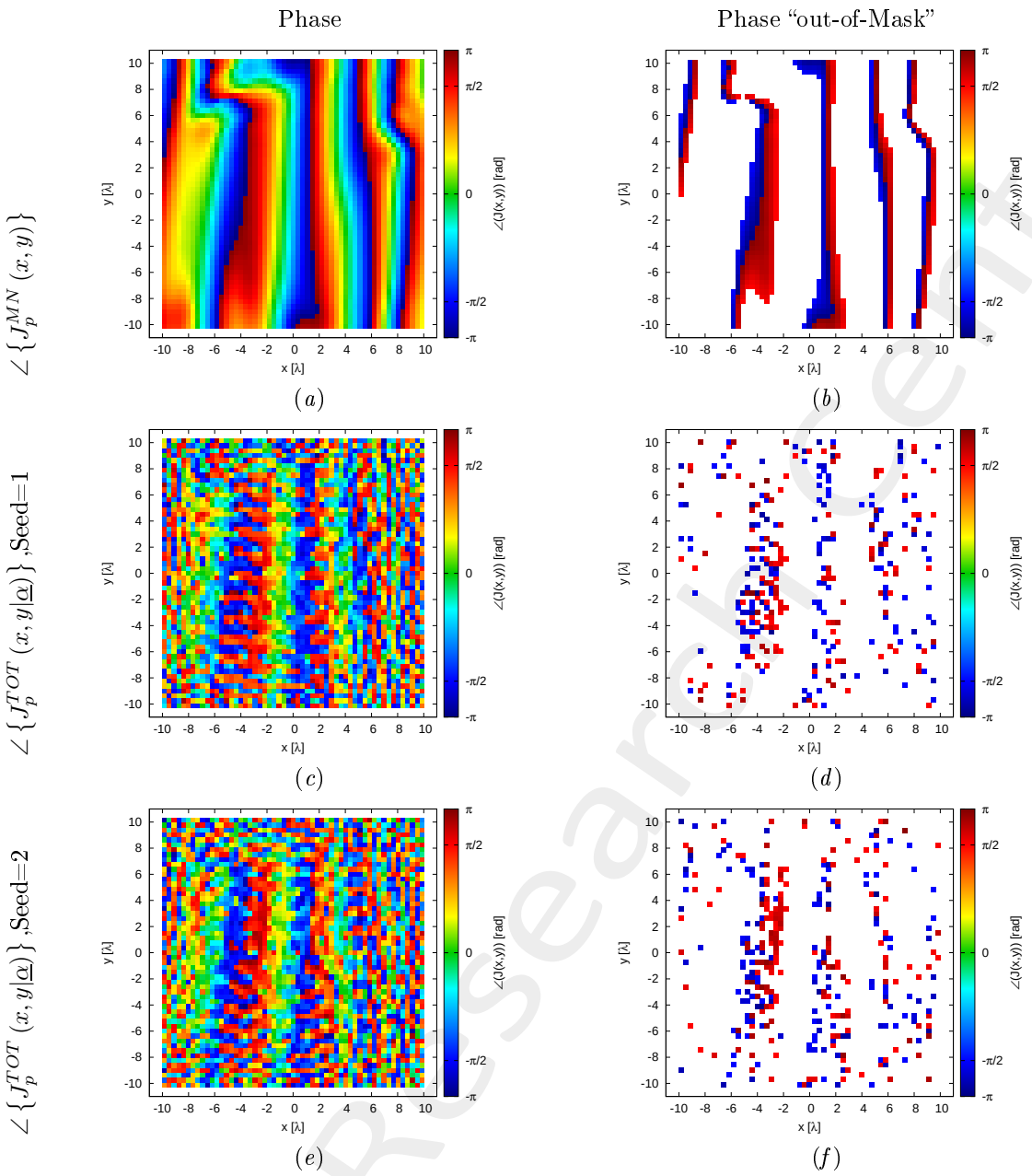


Figure 11: Phase $(a)(c)(e)$ and value of the phase out of the minimization range $(b)(d)(f)$ of the Minimum-Norm current ($\angle\{J_p^{MN}(x,y)\}$)$(a)(b)$, of the total current for the random seed $= 1(c)(d)$ and for the random seed $= 2(e)(f)$.

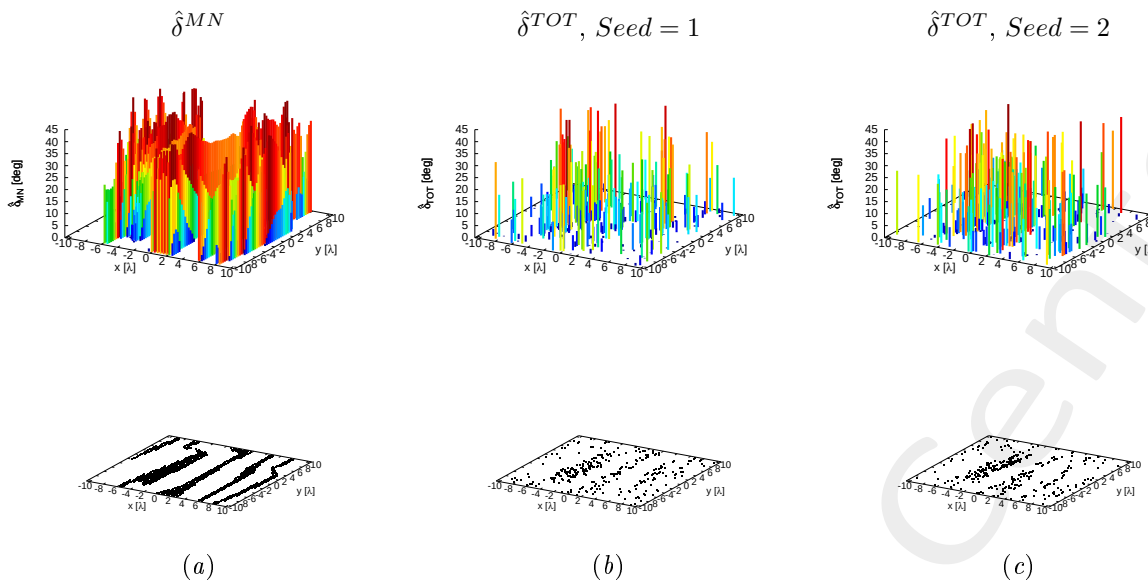


$(a)$ $(b)$ $(c)$

Figure 12: Phase Mask mismatch for the Minimum-Norm current $(a)$, the total current for the random seed $= 1(b)$, and for the random seed $= 2(c)$.

| Case | $\Phi$ | Number of value $> \phi_p^{MAX}(x,y)$ | Number of value $< \phi_p^{MIN}(x,y)$ | Phase Range | | Time $[s]$ |
|---|---|---|---|---|---|---|
| | | | | Min $[deg]$ | Max $[deg]$ | |
| $MN$ | 1.0 | 451 | 358 | $-179.87$ | 179.63 | |
| Seed=1 | $1.919 \times 10^{-1}$ | 148 | 165 | $-178.42$ | 178.19 | $2.09 \times 10^5$ |
| Seed=2 | $2.329 \times 10^{-1}$ | 177 | 157 | $-179.25$ | 177.57 | $1.11 \times 10^5$ |

Table VII: Cost Function value and statistics about the result.

The verification of the radiated field is showed in Fig. 13 and numerically in table VIII.

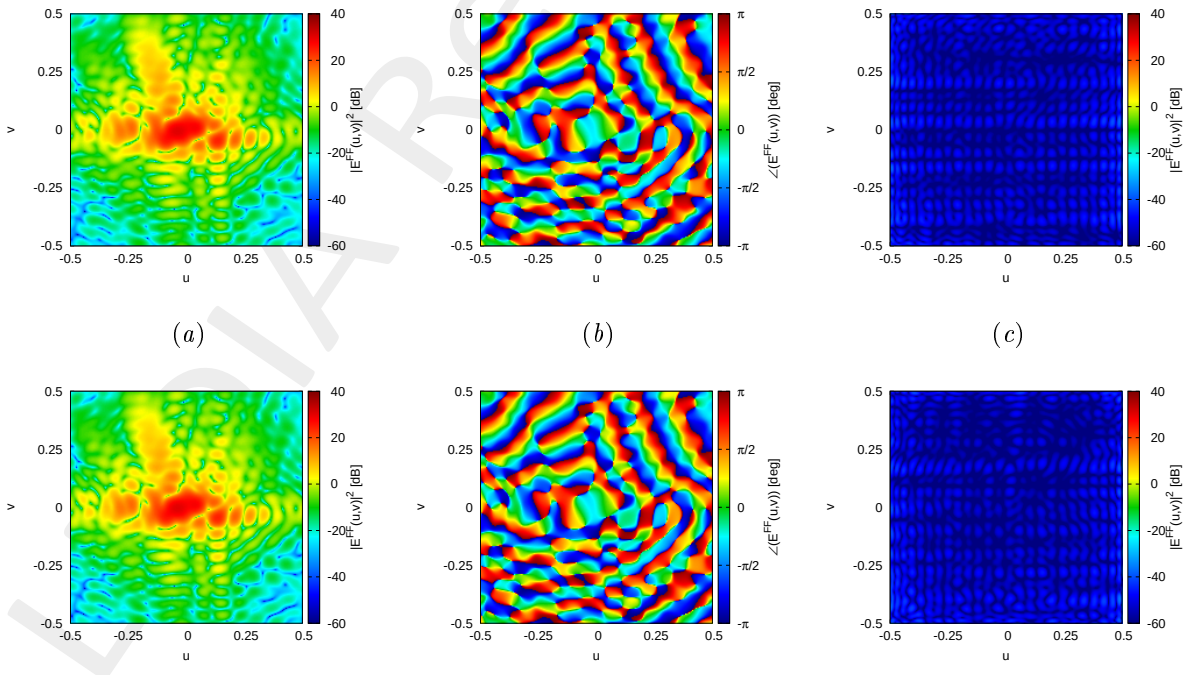


$(a)$ $(b)$ $(c)$

$(d)$ $(e)$ $(f)$

Figure 13: Magnitude $(a)(d)$, Phase $(b)(e)$ and Magnitude of the difference with respect to the original field $(c)(f)$ of the seed=1 $(a)(b)(c)$ and seed=2 $(d)(e)(f)$.

| Seed | $\xi$ |
|---|---|
| 1 | $1.73 \times 10^{-3}$ |
| 2 | $1.67 \times 10^{-3}$ |

Table VIII: Integral error of the difference between the original field and the one radiated by the total current.

## 1.6 K=400, P=100, I=100000

In the Fig. 14 is depicted the behaviour of the Cost Function varying the random seed. The best value of cost function is achieved by Seed=1 and is $\Phi = 2.089 \times 10^{-1}$.

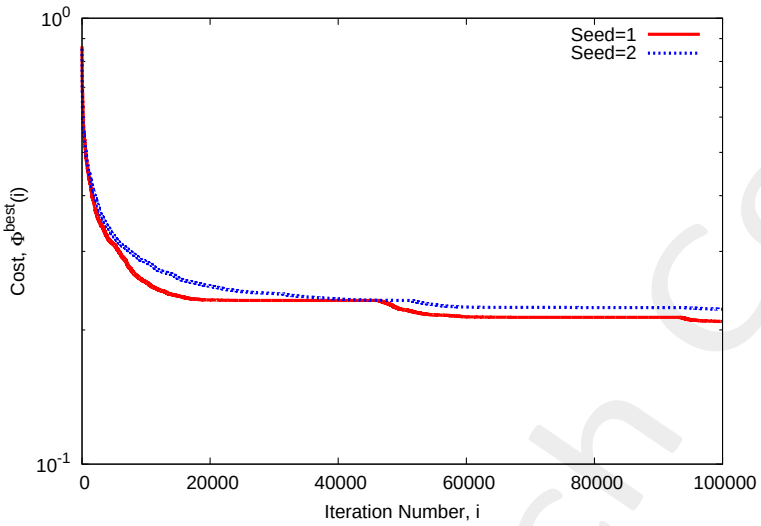


Figure 14: Cost Function behaviour at different random seed.

At this value of cost function the achieved performance on the Phase are showed in Fig. 15 and are numerically showed in table IX.

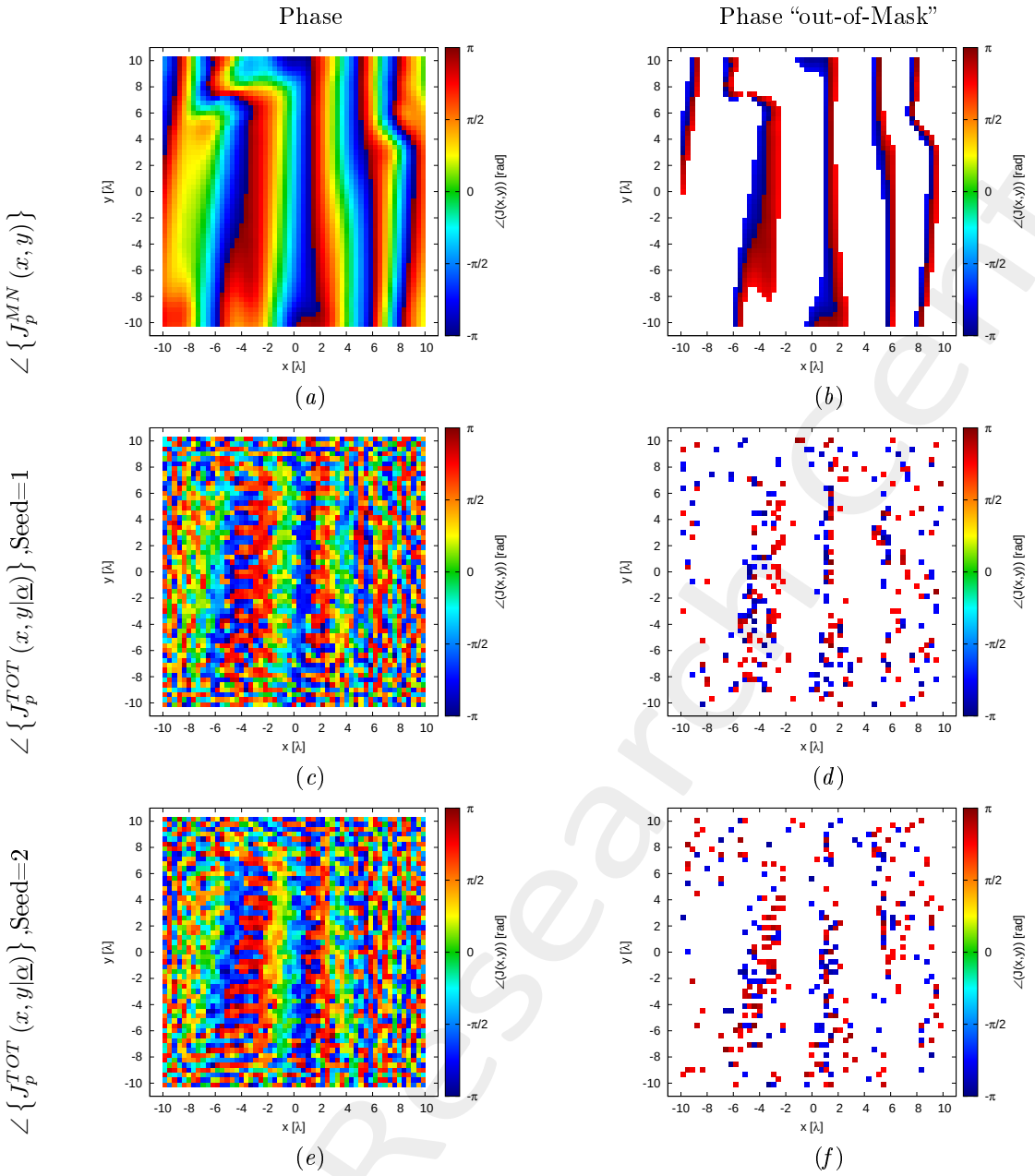


Figure 15: Phase $(a)(c)(e)$ and value of the phase out of the minimization range $(b)(d)(f)$ of the Minimum-Norm current $(\angle\{J_p^{MN}(x,y)\})(a)(b)$, of the total current for the random seed $= 1(c)(d)$ and for the random seed $= 2(e)(f)$.

| Case | $\Phi$ | Number of value $> \phi_p^{MAX}(x,y)$ | Number of value $< \phi_p^{MIN}(x,y)$ | Phase Range | | Time $[s]$ |
|---|---|---|---|---|---|---|
| | | | | Min $[deg]$ | Max $[deg]$ | |
| $MN$ | 1.0 | 451 | 358 | $-179.87$ | 179.63 | |
| Seed=1 | $2.089 \times 10^{-1}$ | 167 | 161 | $-179.91$ | 177.93 | $1.06 \times 10^5$ |
| Seed=2 | $2.225 \times 10^{-1}$ | 186 | 137 | $-175.59$ | 178.64 | $1.08 \times 10^5$ |

Table IX: Cost Function value and statistics about the result.

The verification of the radiated field is showed in Fig. 16 and numerically in table X.

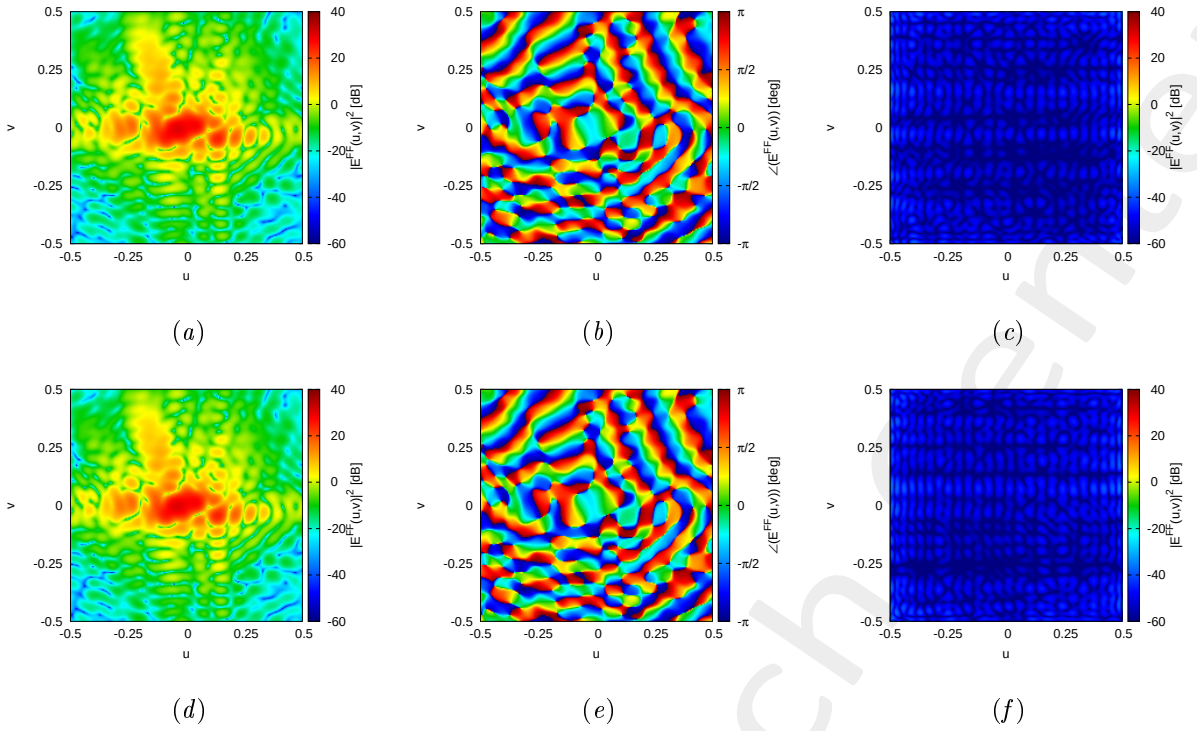


Figure 16: Magnitude $(a)(d)$, Phase $(b)(e)$ and Magnitude of the difference with respect to the original field $(c)(f)$ of the seed=1 $(a)(b)(c)$ and seed=2 $(d)(e)(f)$.

| Seed | $\xi$ |
|---|---|
| 1 | $1.85 \times 10^{-3}$ |
| 2 | $2.02 \times 10^{-3}$ |

Table X: Integral error of the difference between the original field and the one radiated by the total current.

## 1.7 K=400, P=200, I=100000

In the Fig. 17 is depicted the behaviour of the Cost Function varying the random seed. The best value of cost function is achieved by Seed=1 and is $\Phi = 2.211 \times 10^{-1}$.

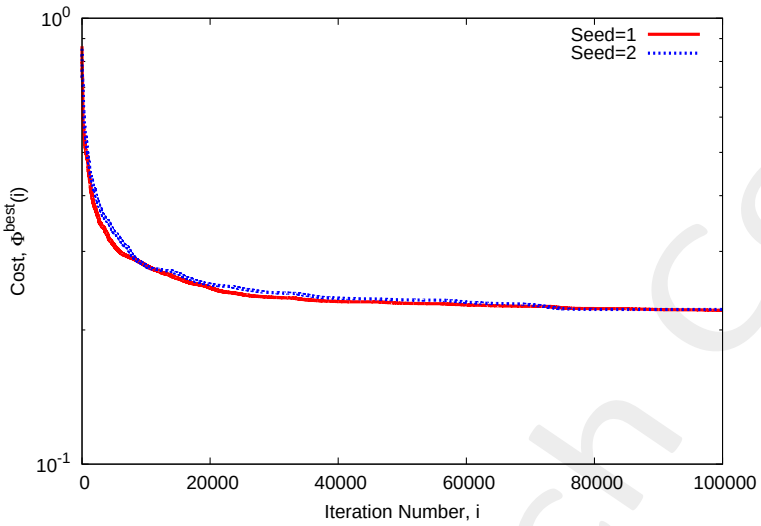


Figure 17: Cost Function behaviour at different random seed.

At this value of cost function the achieved performance on the Phase are showed in Fig. 18 and are numerically showed in table XI.

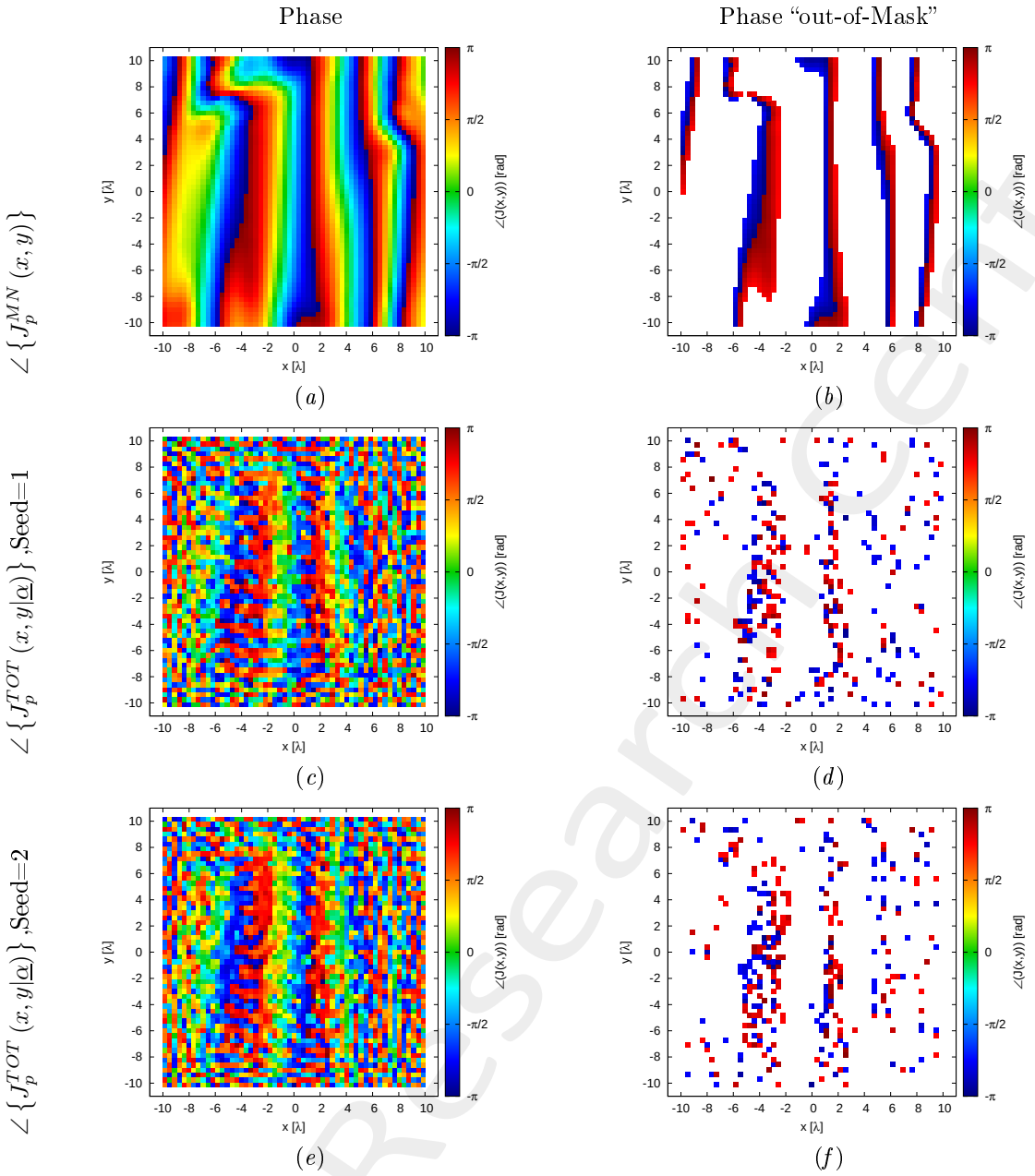


Figure 18: Phase $(a)(c)(e)$ and value of the phase out of the minimization range $(b)(d)(f)$ of the Minimum-Norm current ($\angle\{J_p^{MN}(x,y)\}$)$(a)(b)$, of the total current for the random seed $= 1(c)(d)$ and for the random seed $= 2(e)(f)$.

| Case | $\Phi$ | Number of value $> \phi_p^{MAX}(x,y)$ | Number of value $< \phi_p^{MIN}(x,y)$ | Phase Range | | Time $[s]$ |
|---|---|---|---|---|---|---|
| | | | | Min $[deg]$ | Max $[deg]$ | |
| $MN$ | 1.0 | 451 | 358 | $-179.87$ | 179.63 | |
| Seed=1 | $2.211 \times 10^{-1}$ | 171 | 155 | $-179.95$ | 178.50 | $2.24 \times 10^5$ |
| Seed=2 | $2.222 \times 10^{-1}$ | 179 | 153 | $-178.96$ | 177.78 | $2.19 \times 10^5$ |

Table XI: Cost Function value and statistics about the result.

The verification of the radiated field is showed in Fig. 19 and numerically in table XII.

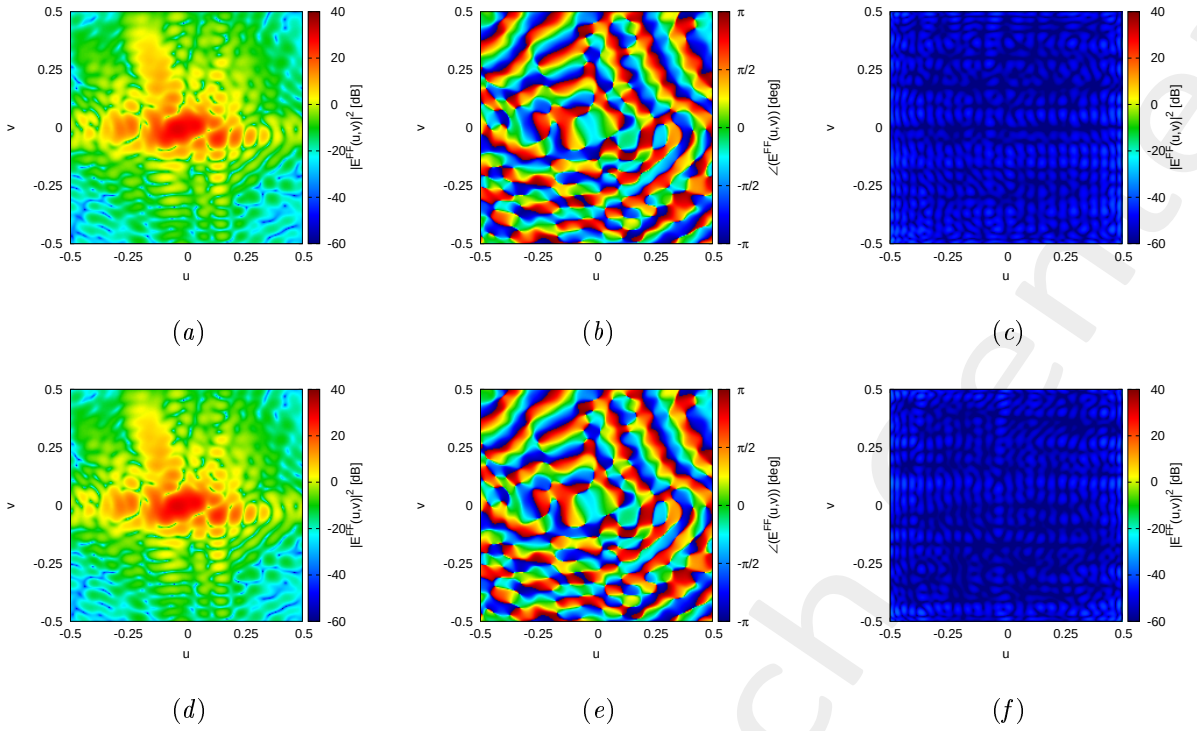


Figure 19: Magnitude $(a)(d)$, Phase $(b)(e)$ and Magnitude of the difference with respect to the original field $(c)(f)$ of the seed=1 $(a)(b)(c)$ and seed=2 $(d)(e)(f)$.

| Seed | $\xi$ |
|---|---|
| 1 | $2.09 \times 10^{-3}$ |
| 2 | $1.81 \times 10^{-3}$ |

Table XII: Integral error of the difference between the original field and the one radiated by the total current.

## 1.8 K=800, P=100, I=100000

In the Fig. 20 is depicted the behaviour of the Cost Function varying the random seed. The best value of cost function is achieved by Seed=2 and is $\Phi = 1.697 \times 10^{-1}$.

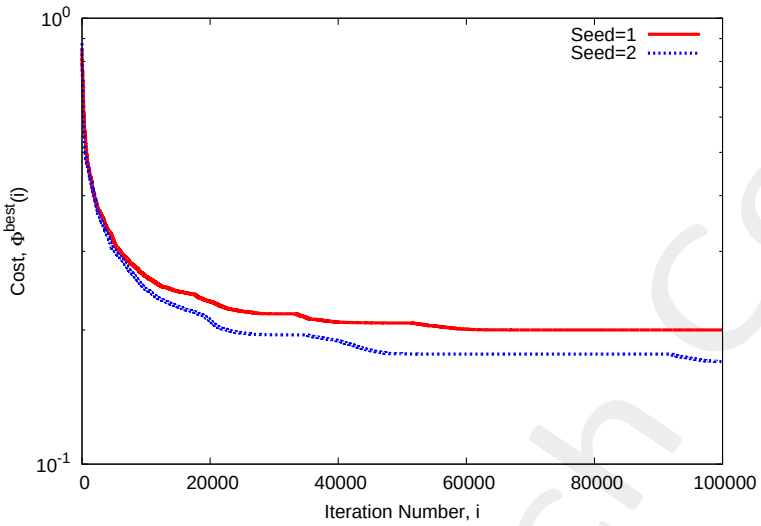


Figure 20: Cost Function behaviour at different random seed.

At this value of cost function the achieved performance on the Phase are showed in Fig. 21 and are numerically showed in table XIII.

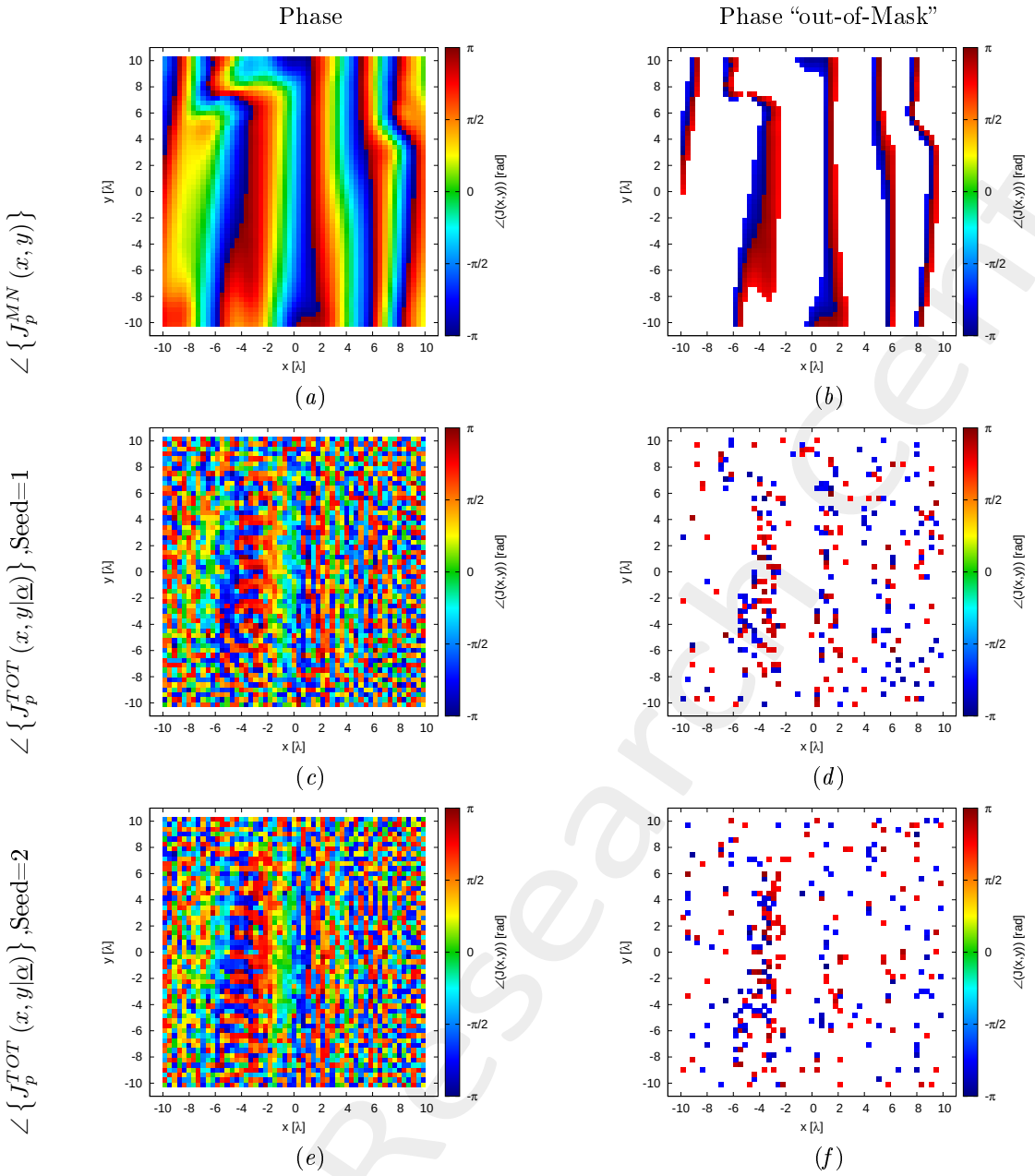


Figure 21: Phase $(a)(c)(e)$ and value of the phase out of the minimization range $(b)(d)(f)$ of the Minimum-Norm current ($\angle\{J_p^{MN}(x,y)\}$)$(a)(b)$, of the total current for the random seed $= 1(c)(d)$ and for the random seed $= 2(e)(f)$.

| Case | $\Phi$ | Number of value $> \phi_p^{MAX}(x,y)$ | Number of value$< \phi_p^{MIN}(x,y)$ | Phase Range | | Time $[s]$ |
|---|---|---|---|---|---|---|
| | | | | Min $[deg]$ | Max $[deg]$ | |
| $MN$ | 1.0 | 451 | 358 | $-179.87$ | 179.63 | |
| Seed=1 | $1.999 \times 10^{-1}$ | 151 | 149 | $-178.85$ | 177.20 | $2.27 \times 10^5$ |
| Seed=2 | $1.697 \times 10^{-1}$ | 143 | 139 | $-178.59$ | 178.00 | $2.12 \times 10^5$ |

Table XIII: Cost Function value and statistics about the result.

The verification of the radiated field is showed in Fig. 22 and numerically in table XIV.

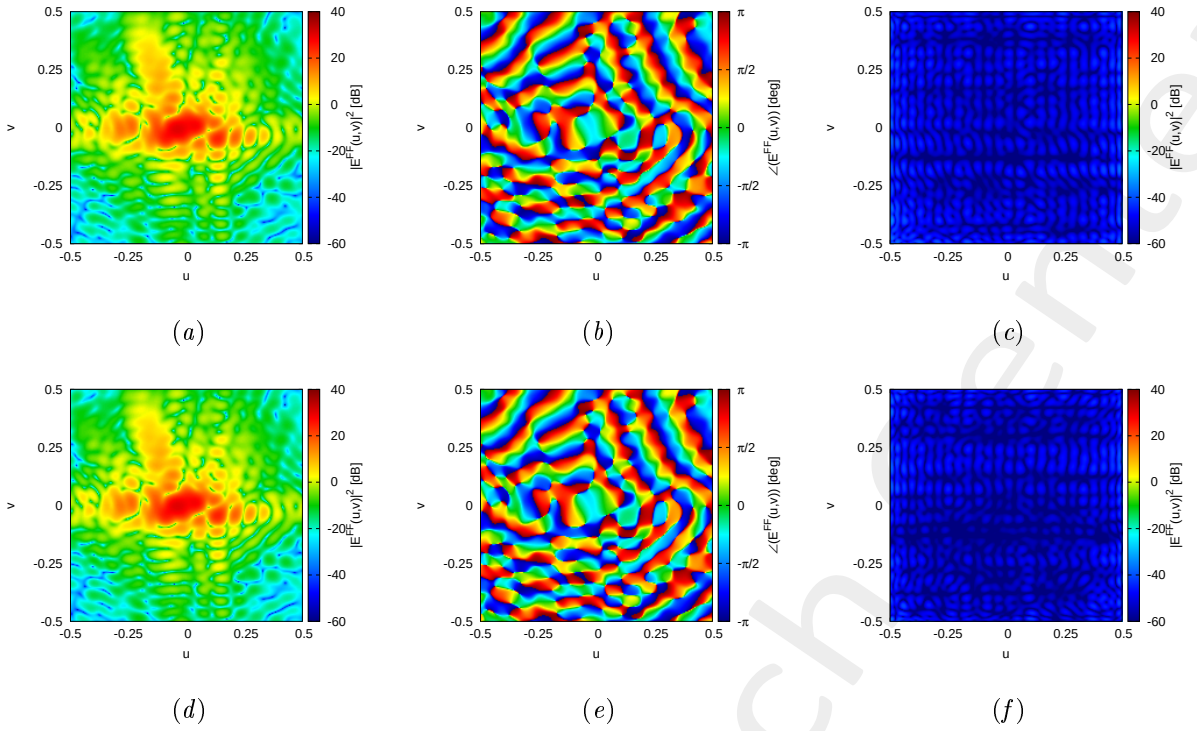


Figure 22: Magnitude $(a)(d)$, Phase $(b)(e)$ and Magnitude of the difference with respect to the original field $(c)(f)$ of the seed=1 $(a)(b)(c)$ and seed=2 $(d)(e)(f)$.

| Seed | $\xi$ |
|---|---|
| 1 | $2.20 \times 10^{-3}$ |
| 2 | $1.82 \times 10^{-3}$ |

Table XIV: Integral error of the difference between the original field and the one radiated by the total current.

## 1.9 K=800, P=200, I=100000

In the Fig. 23 is depicted the behaviour of the Cost Function varying the random seed. The best value of cost function is achieved by Seed=1 and is $\Phi = 1.161 \times 10^{-1}$.

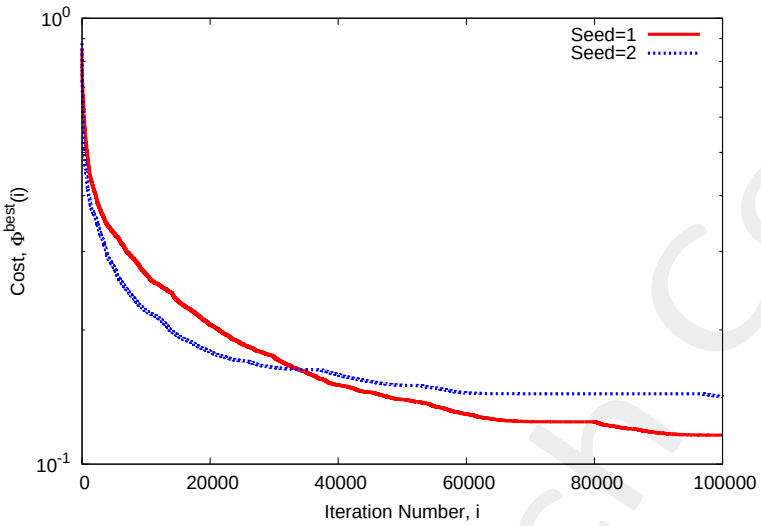


Figure 23: Cost Function behaviour at different random seed.

At this value of cost function the achieved performance on the Phase are showed in Fig. 24 and are numerically showed in table XV.

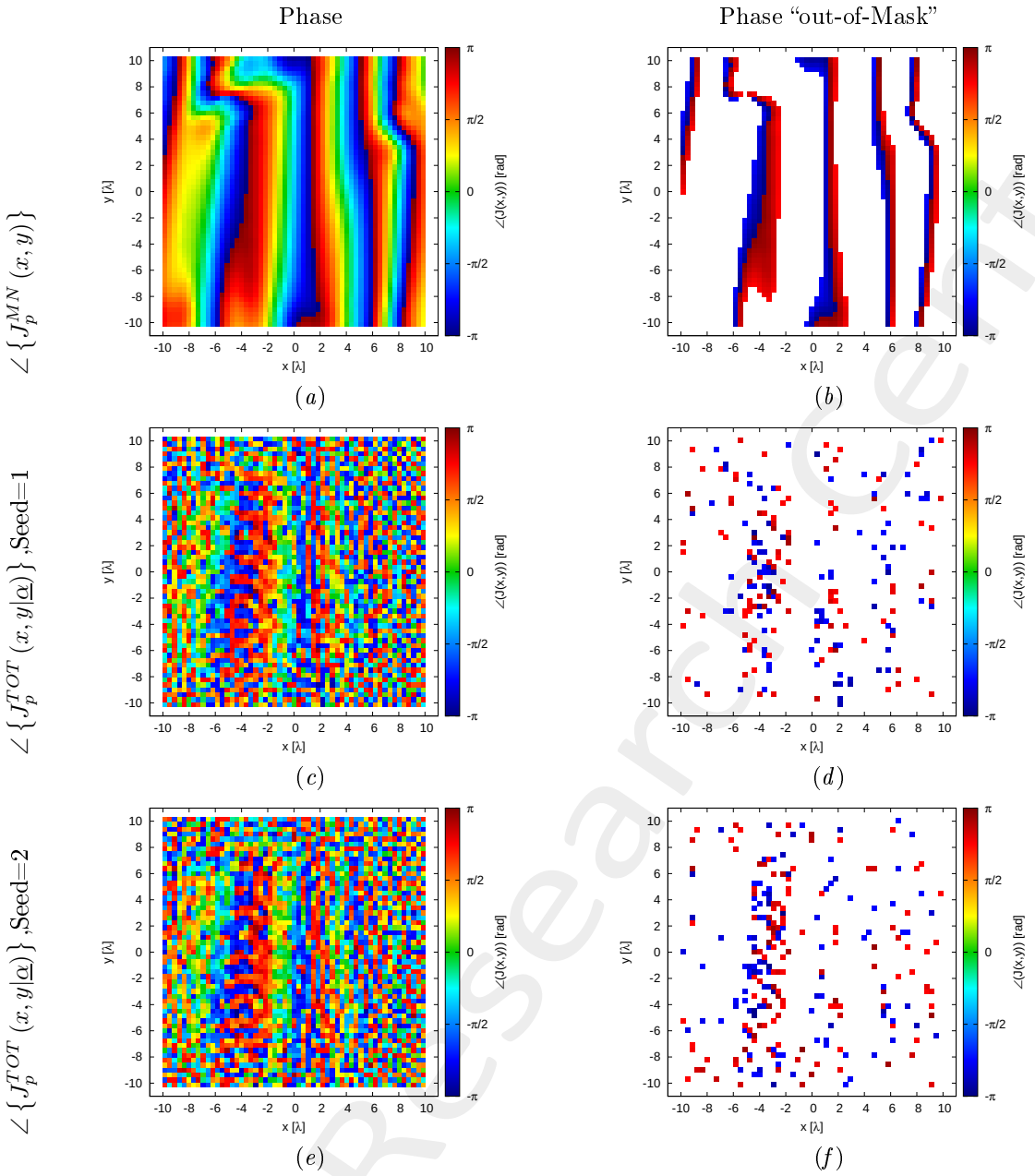


Figure 24: Phase $(a)(c)(e)$ and value of the phase out of the minimization range $(b)(d)(f)$ of the Minimum-Norm current ($\angle\{J_p^{MN}(x,y)\}$)$(a)(b)$, of the total current for the random seed $= 1(c)(d)$ and for the random seed $= 2(e)(f)$.

| Case | $\Phi$ | Number of value $> \phi_p^{MAX}(x,y)$ | Number of value$< \phi_p^{MIN}(x,y)$ | Phase Range | | Time $[s]$ |
|---|---|---|---|---|---|---|
| | | | | Min $[deg]$ | Max $[deg]$ | |
| $MN$ | 1.0 | 451 | 358 | $-179.87$ | 179.63 | |
| Seed=1 | $1.161 \times 10^{-1}$ | 108 | 102 | $-175.79$ | 178.84 | $4.20 \times 10^5$ |
| Seed=2 | $1.416 \times 10^{-1}$ | 130 | 113 | $-178.22$ | 175.86 | $4.27 \times 10^5$ |

Table XV: Cost Function value and statistics about the result.

The verification of the radiated field is showed in Fig. 25 and numerically in table XVI.

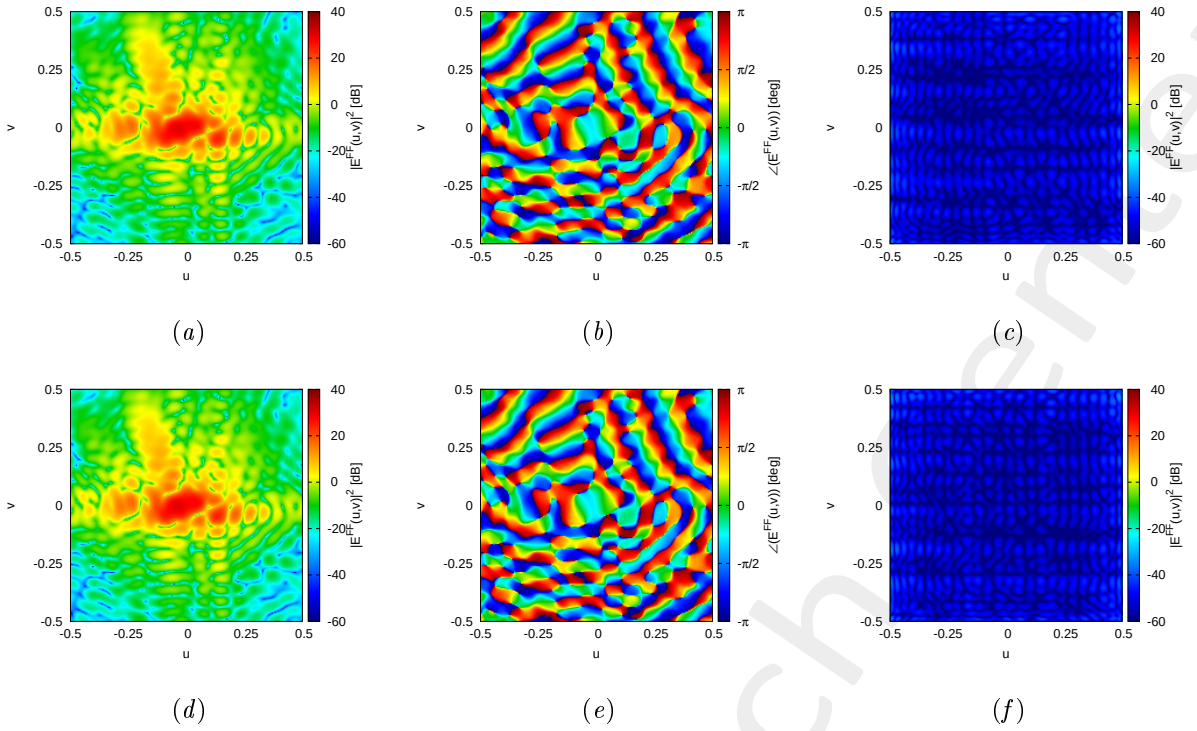


Figure 25: Magnitude $(a)(d)$, Phase $(b)(e)$ and Magnitude of the difference with respect to the original field $(c)(f)$ of the seed=1 $(a)(b)(c)$ and seed=2 $(d)(e)(f)$.

| Seed | $\xi$ |
|---|---|
| 1 | $2.02 \times 10^{-3}$ |
| 2 | $1.98 \times 10^{-3}$ |

Table XVI: Integral error of the difference between the original field and the one radiated by the total current.

## 1.10 K=800, P=400, I=100000

In the Fig. 26 is depicted the behaviour of the Cost Function varying the random seed. The best value of cost function is achieved by Seed=2 and is $\Phi = 9.787 \times 10^{-2}$.

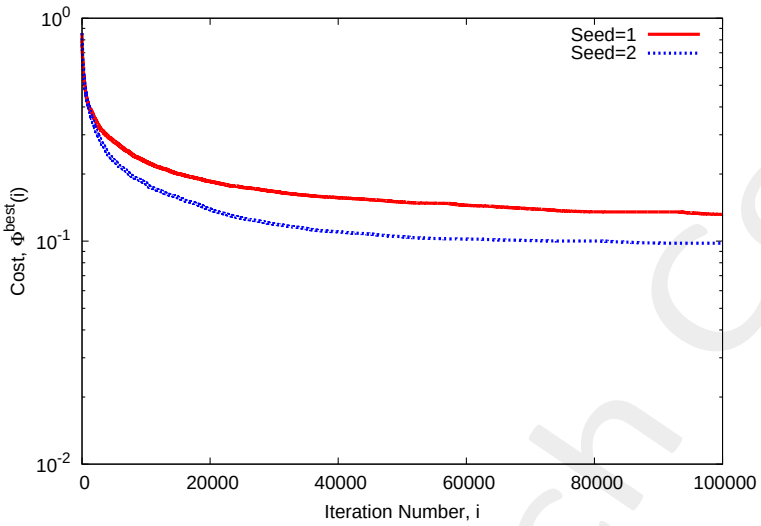


Figure 26: Cost Function behaviour at different random seed.

At this value of cost function the achieved performance on the Phase are showed in Fig. 27 and are numerically showed in table XVII.

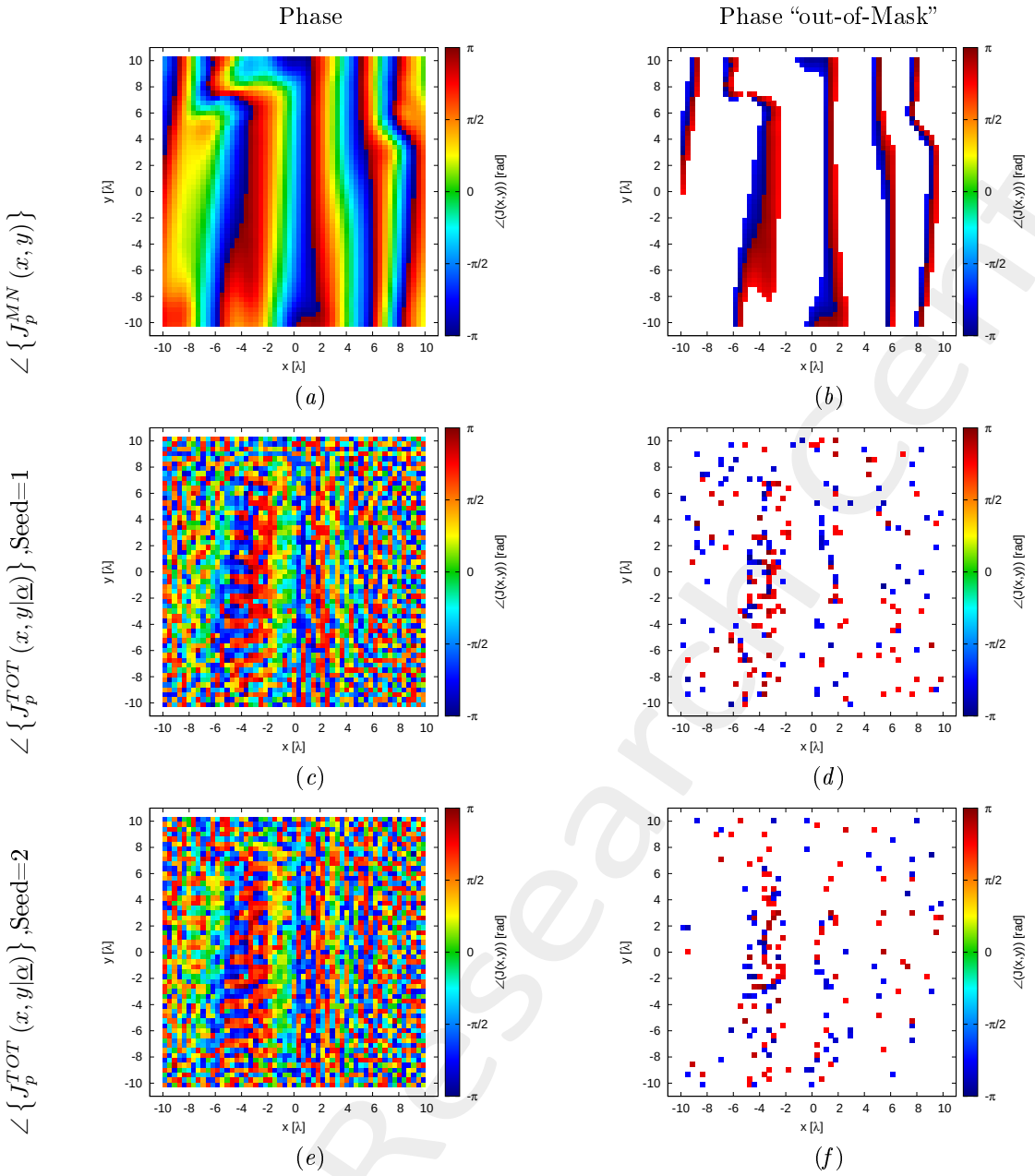


Figure 27: Phase $(a)(c)(e)$ and value of the phase out of the minimization range $(b)(d)(f)$ of the Minimum-Norm current $(\angle\{J_p^{MN}(x,y)\})(a)(b)$, of the total current for the random seed $= 1(c)(d)$ and for the random seed $= 2(e)(f)$.

| Case | $\Phi$ | Number of value $> \phi_p^{MAX}(x,y)$ | Number of value$< \phi_p^{MIN}(x,y)$ | Phase Range | | Time $[s]$ |
|---|---|---|---|---|---|---|
| | | | | Min $[deg]$ | Max $[deg]$ | |
| $MN$ | 1.0 | 451 | 358 | $-179.87$ | 179.63 | |
| Seed=1 | $1.318 \times 10^{-1}$ | 120 | 117 | $-176.27$ | 178.12 | $8.70 \times 10^5$ |
| Seed=2 | $9.787 \times 10^{-2}$ | 94 | 85 | $-173.11$ | 179.11 | $8.75 \times 10^5$ |

Table XVII: Cost Function value and statistics about the result.

The verification of the radiated field is showed in Fig. 28 and numerically in table XVIII.

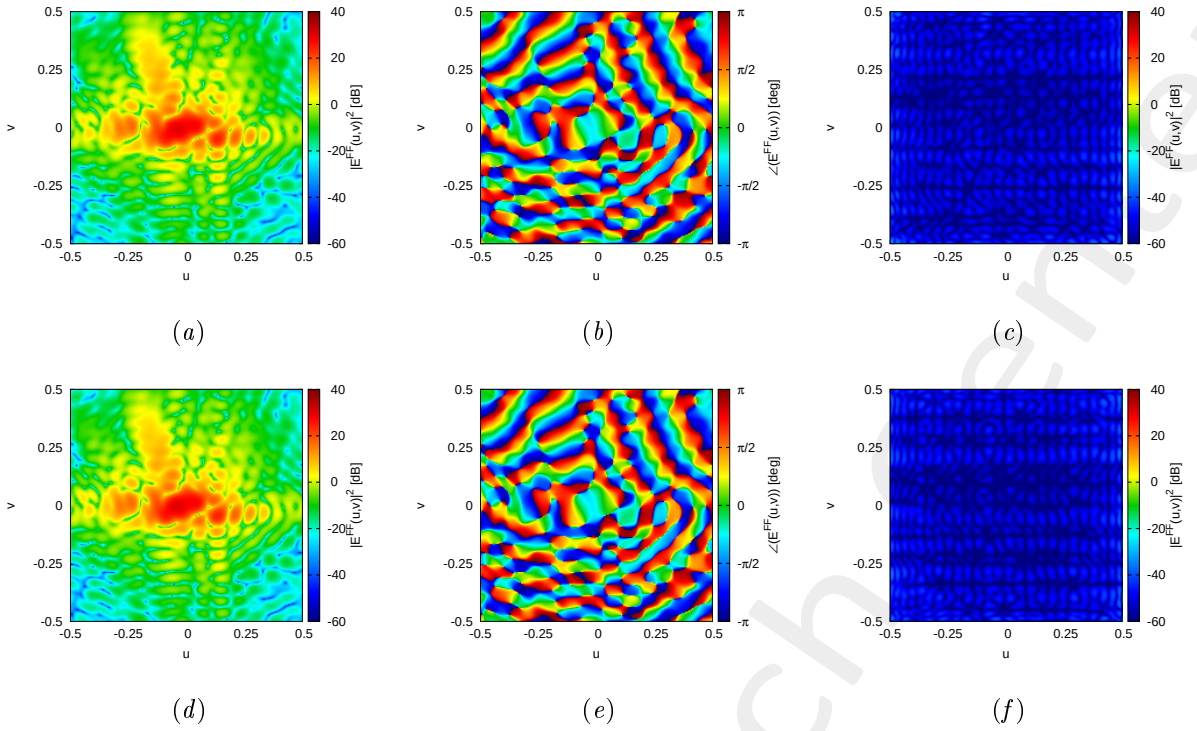


Figure 28: Magnitude $(a)(d)$, Phase $(b)(e)$ and Magnitude of the difference with respect to the original field $(c)(f)$ of the seed=1 $(a)(b)(c)$ and seed=2 $(d)(e)(f)$.

| Seed | $\xi$ |
|---|---|
| 1 | $2.01 \times 10^{-3}$ |
| 2 | $2.02 \times 10^{-3}$ |

Table XVIII: Integral error of the difference between the original field and the one radiated by the total current.

## 1.11 K=800, P=160, I=300000

In the Fig. 29 is depicted the behaviour of the Cost Function varying the random seed. The best value of cost function is achieved by Seed=2 and is $\Phi = 8.129 \times 10^{-2}$.

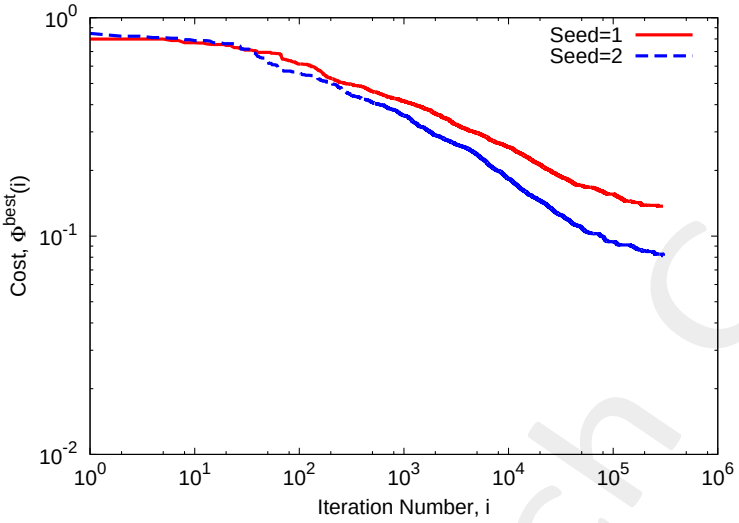


Figure 29: Cost Function behaviour at different random seed.

At this value of cost function the achieved performance on the Phase are showed in Fig. 30 and are numerically showed in table XIX.

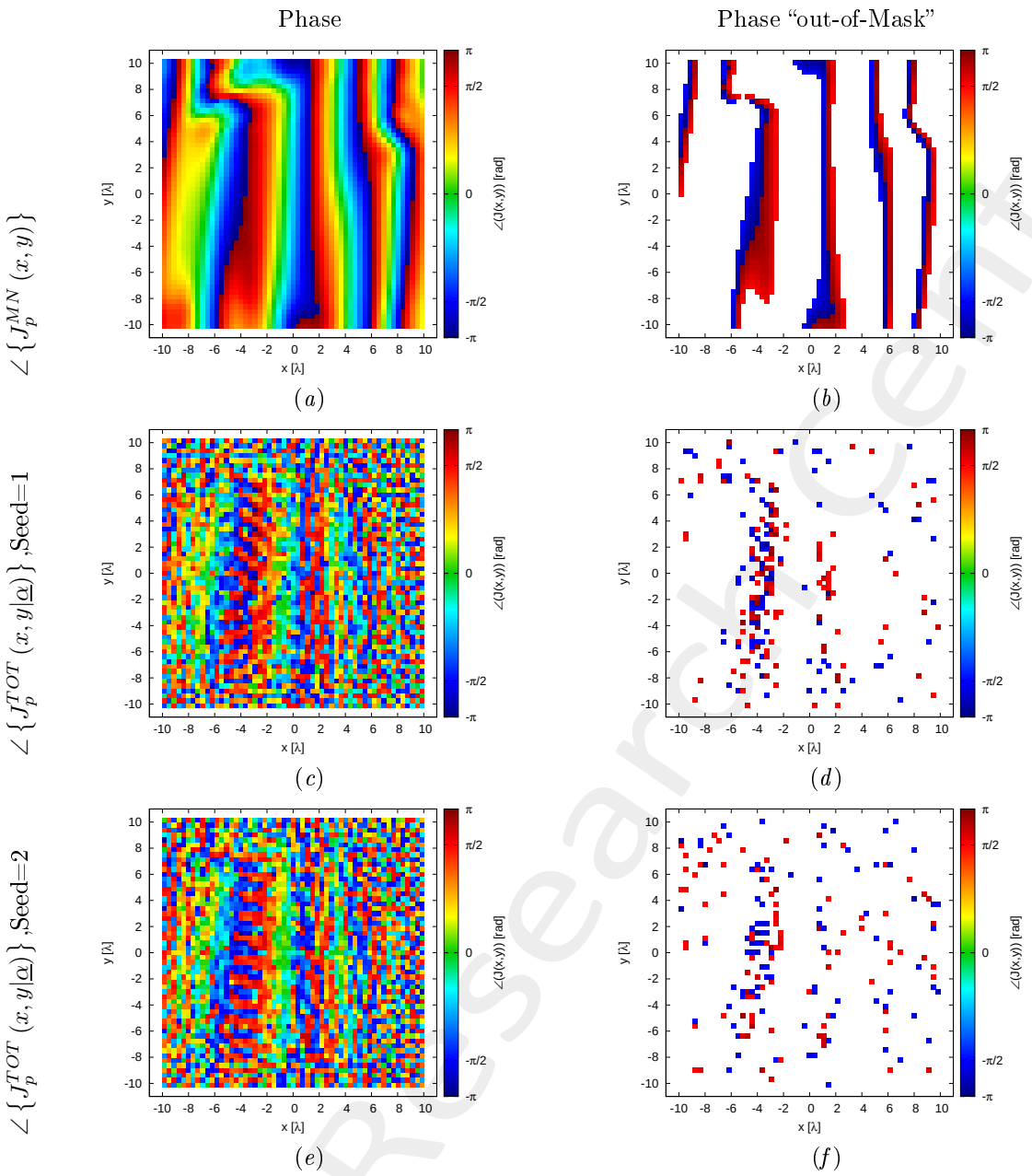


Figure 30: Phase $(a)(c)(e)$ and value of the phase out of the minimization range $(b)(d)(f)$ of the Minimum-Norm current ($\angle\{J_p^{MN}(x,y)\}$)$(a)(b)$, of the total current for the random seed $= 1(c)(d)$ and for the random seed $= 2(e)(f)$.

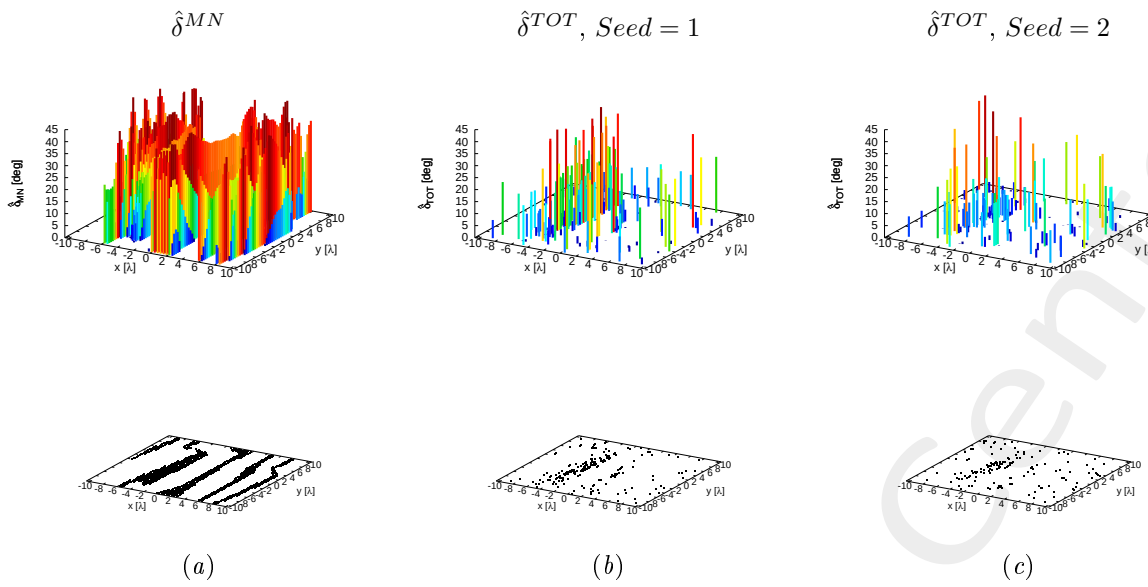


$(a)$ $(b)$ $(c)$

Figure 31: Phase Mask mismatch for the Minimum-Norm current $(a)$, the total current for the random seed $= 1(b)$, and for the random seed $= 2(c)$.

| Case | $\Phi$ | Number of value $> \phi_p^{MAX}(x,y)$ | Number of value $< \phi_p^{MIN}(x,y)$ | Phase Range | | Time $[s]$ |
|---|---|---|---|---|---|---|
| | | | | Min $[deg]$ | Max $[deg]$ | |
| $MN$ | 1.0 | 451 | 358 | $-179.87$ | 179.63 | |
| Seed=1 | $1.369 \times 10^{-1}$ | 114 | 95 | $-179.25$ | 177.18 | $3.86 \times 10^5$ |
| Seed=2 | $8.129 \times 10^{-2}$ | 94 | 90 | $-178.78$ | 173.59 | $1.50 \times 10^5$ |

Table XIX: Cost Function value and statistics about the result.

The verification of the radiated field is showed in Fig. 32 and numerically in table XX.

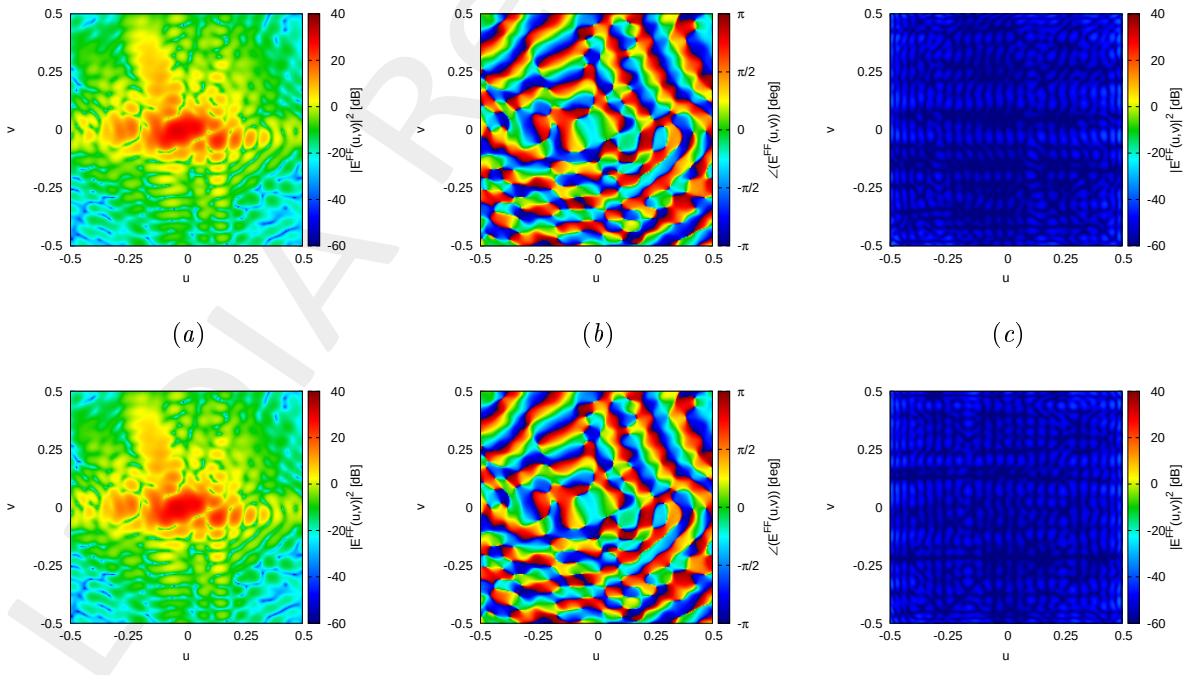


$(a)$ $(b)$ $(c)$

$(d)$ $(e)$ $(f)$

Figure 32: Magnitude $(a)(d)$, Phase $(b)(e)$ and Magnitude of the difference with respect to the original field $(c)(f)$ of the seed=1 $(a)(b)(c)$ and seed=2 $(d)(e)(f)$.

| Seed | $\xi$ |
|---|---|
| 1 | $1.75 \times 10^{-3}$ |
| 2 | $1.82 \times 10^{-3}$ |

Table XX: Integral error of the difference between the original field and the one radiated by the total current.

**More information on the topics of this document can be found in the following list of references.**

## References


[1] M. Salucci, G. Oliveri, M. A. Hannan, and A. Massa, "System-by-design paradigm-based synthesis of complex systems: The case of spline-contoured 3D radomes," *IEEE Antennas and Propagation Magazine - Special Issue on 'Artificial Intelligence in Electromagnetics,'*, vol. 64, no. 1, pp. 72-83, Feb. 2022.

[2] G. Oliveri, P. Rocca, M. Salucci, and A. Massa, "Holographic smart EM skins for advanced beam power shaping in next generation wireless environments," *IEEE J. Multiscale Multiphysics Comput. Tech.*, vol. 6, pp. 171-182, Oct. 2021.

[3] G. Oliveri, A. Gelmini, A. Polo, N. Anselmi, and A. Massa, "System-by-design multi-scale synthesis of task-oriented reflectarrays," *IEEE Trans. Antennas Propag.*, vol. 68, no. 4, pp. 2867-2882, Apr. 2020.

[4] M. Salucci, L. Tenuti, G. Gottardi, A. Hannan, and A. Massa, "System-by-design method for efficient linear array miniaturisation through low-complexity isotropic lenses," *Electronic Letters*, vol. 55, no. 8, pp. 433-434, May 2019.

[5] M. Salucci, N. Anselmi, S. Goudos, and A. Massa, "Fast design of multiband fractal antennas through a system-by-design approach for NB-IoT applications," *EURASIP J. Wirel. Commun. Netw.*, vol. 2019, no. 1, pp. 68-83, Mar. 2019.

[6] M. Salucci, G. Oliveri, N. Anselmi, and A. Massa, "Material-by-design synthesis of conformal miniaturized linear phased arrays," *IEEE Access*, vol. 6, pp. 26367-26382, 2018.

[7] M. Salucci, G. Oliveri, N. Anselmi, G. Gottardi, and A. Massa, "Performance enhancement of linear active electronically-scanned arrays by means of MbD-synthesized metalenses," *Journal of Electromagnetic Waves and Applications*, vol. 32, no. 8, pp. 927-955, 2018.

[8] G. Oliveri, M. Salucci, N. Anselmi and A. Massa, "Multiscale System-by-Design synthesis of printed WAIMs for waveguide array enhancement," *IEEE J. Multiscale Multiphysics Computat. Techn.*, vol. 2, pp. 84-96, 2017.

[9] A. Massa and G. Oliveri, "Metamaterial-by-Design: Theory, methods, and applications to communications and sensing - Editorial," *EPJ Applied Metamaterials*, vol. 3, no. E1, pp. 1-3, 2016.

[10] G. Oliveri, F. Viani, N. Anselmi, and A. Massa, "Synthesis of multi-layer WAIM coatings for planar phased arrays within the system-by-design framework," *IEEE Trans. Antennas Propag.*, vol. 63, no. 6, pp. 2482-2496, June 2015.

[11] G. Oliveri, L. Tenuti, E. Bekele, M. Carlin, and A. Massa, "An SbD-QCTO approach to the synthesis of isotropic metamaterial lenses," *IEEE Antennas Wireless Propag. Lett.*, vol. 13, pp. 1783-1786, 2014.

[12] A. Massa, G. Oliveri, P. Rocca, and F. Viani, "System-by-Design: a new paradigm for handling design complexity," *8th European Conference on Antennas Propag. (EuCAP 2014), The Hague, The Netherlands*, pp. 1180-1183, Apr. 6-11, 2014.

[13] P. Rocca, M. Benedetti, M. Donelli, D. Franceschini, and A. Massa, "Evolutionary optimization as applied to inverse problems," *Inverse Problems - 25 th Year Special Issue of Inverse Problems, Invited Topical Review*, vol. 25, pp. 1-41, Dec. 2009.

[14] P. Rocca, G. Oliveri, and A. Massa, "Differential Evolution as applied to electromagnetics," *IEEE Antennas Propag. Mag.*, vol. 53, no. 1, pp. 38-49, Feb. 2011.

[15] M. Salucci, G. Gottardi, N. Anselmi, and G. Oliveri, "Planar thinned array design by hybrid analytical-stochastic optimization," *IET Microwaves, Antennas & Propagation*, vol. 11, no. 13, pp. 1841-1845, Oct. 2017

[16] G. Oliveri, M. Donelli, and A. Massa, "Genetically-designed arbitrary length almost difference sets," *Electronics Letters*, vol. 5, no. 23, pp. 1182-1183, Nov. 2009.

[17] P. Rocca, N. Anselmi, A. Polo, and A. Massa, "Pareto-optimal domino-tiling of orthogonal polygon phased arrays," *IEEE Trans. Antennas Propag.*, vol. 70, no. 5, pp. 3329-3342, May 2022.

[18] P. Rocca, N. Anselmi, A. Polo, and A. Massa, "An irregular two-sizes square tiling method for the design of isophoric phased arrays," *IEEE Trans. Antennas Propag.*, vol. 68, no. 6, pp. 4437-4449, Jun. 2020.

[19] P. Rocca, N. Anselmi, A. Polo, and A. Massa, "Modular design of hexagonal phased arrays through diamond tiles," *IEEE Trans. Antennas Propag.*, vol.68, no. 5, pp. 3598-3612, May 2020.

[20] N. Anselmi, L. Poli, P. Rocca, and A. Massa, "Design of simplified array layouts for preliminary experimental testing and validation of large AESAs," *IEEE Trans. Antennas Propag.*, vol. 66, no. 12, pp. 6906-6920, Dec. 2018.

[21] N. Anselmi, P. Rocca, M. Salucci, and A. Massa, "Contiguous phase-clustering in multibeam-on-receive scanning arrays," *IEEE Trans. Antennas Propag.*, vol. 66, no. 11, pp. 5879-5891, Nov. 2018.

[22] G. Oliveri, G. Gottardi, F. Robol, A. Polo, L. Poli, M. Salucci, M. Chuan, C. Massagrande, P. Vinetti, M. Mattivi, R. Lombardi, and A. Massa, "Co-design of unconventional array architectures and antenna elements for 5G base station," *IEEE Trans. Antennas Propag.*, vol. 65, no. 12, pp. 6752-6767, Dec. 2017.

[23] N. Anselmi, P. Rocca, M. Salucci, and A. Massa, "Irregular phased array tiling by means of analytic schemata-driven optimization," *IEEE Trans. Antennas Propag.*, vol. 65, no. 9, pp. 4495-4510, September 2017.

[24] N. Anselmi, P. Rocca, M. Salucci, and A. Massa, "Optimization of excitation tolerances for robust beamforming in linear arrays," *IET Microwaves, Antennas & Propagation*, vol. 10, no. 2, pp. 208-214, 2016.

[25] P. Rocca, R. J. Mailloux, and G. Toso, "GA-Based optimization of irregular sub-array layouts for wideband phased arrays desig," *IEEE Antennas and Wireless Propag. Lett.*, vol. 14, pp. 131-134, 2015.

[26] P. Rocca, M. Donelli, G. Oliveri, F. Viani, and A. Massa, "Reconfigurable sum-difference pattern by means of parasitic elements for forward-looking monopulse radar," *IET Radar, Sonar & Navigation*, vol 7, no. 7, pp. 747-754, 2013.

[27] P. Rocca, L. Manica, and A. Massa, "Ant colony based hybrid approach for optimal compromise sum-difference patterns synthesis," *Microwave Opt. Technol. Lett.*, vol. 52, no. 1, pp. 128-132, Jan. 2010.

[28] P. Rocca, L. Manica, and A. Massa, "An improved excitation matching method based on an ant colony optimization for suboptimal-free clustering in sum-difference compromise synthesis," *IEEE Trans. Antennas Propag.*, vol. 57, no. 8, pp. 2297-2306, Aug. 2009.

[29] P. Rocca, L. Manica, and A. Massa, "Hybrid approach for sub-arrayed monopulse antenna synthesis," *Electronics Letters*, vol. 44, no. 2, pp. 75-76, Jan. 2008.

[30] P. Rocca, L. Manica, F. Stringari, and A. Massa, "Ant colony optimization for tree-searching based synthesis of monopulse array antenna," *Electronics Letters*, vol. 44, no. 13, pp. 783-785, Jun. 19, 2008.

[31] M. Salucci, F. Robol, N. Anselmi, M. A. Hannan, P. Rocca, G. Oliveri, M. Donelli, and A. Massa, "S-Band spline-shaped aperture-stacked patch antenna for air traffic control applications," *IEEE Tran. Antennas Propag.*, vol. 66, no. 8, pp. 4292-4297, Aug. 2018.

[32] T. Moriyama, F. Viani, M. Salucci, F. Robol, and E. Giarola, "Planar multiband antenna for 3G/4G advanced wireless services," *IEICE Electronics Express*, vol. 11, no. 17, pp. 1-10, Sep. 2014.

[33] F. Viani, "Dual-band sierpinski pre-fractal antenna for 2.4GHz-WLAN and 800MHz-LTE wireless devices," *Progress In Electromagnetics Research C*, vol. 35, pp. 63-71, 2013.

[34] F. Viani, M. Salucci, F. Robol, and A. Massa, "Multiband fractal Zigbee/WLAN antenna for ubiquitous wireless environments," *Journal of Electromagnetic Waves and Applications*, vol. 26, no. 11-12, pp. 1554-1562. 2012.

[35] F. Viani, M. Salucci, F. Robol, G. Oliveri, and A. Massa, "Design of a UHF RFID/GPS fractal antenna for logistics management," *Journal of Electromagnetic Waves and Applications*, vol. 26, pp. 480-492, 2012.

[36] M. Salucci, L. Poli, A. F. Morabito, and P. Rocca, "Adaptive nulling through subarray switching in planar antenna arrays," *Journal of Electromagnetic Waves and Applications*, vol. 30, no. 3, pp. 404-414, February 2016

[37] T. Moriyama, L. Poli, and P. Rocca, "Adaptive nulling in thinned planar arrays through genetic algorithms," *IEICE Electronics Express*, vol. 11, no. 21, pp. 1-9, Sep. 2014.

[38] L. Poli, P. Rocca, M. Salucci, and A. Massa, "Reconfigurable thinning for the adaptive control of linear arrays," *IEEE Trans. Antennas Propag.*, vol. 61, no. 10, pp. 5068-5077, Oct. 2013.

[39] P. Rocca, L. Poli, G. Oliveri, and A. Massa, "Adaptive nulling in time-varying scenarios through time-modulated linear arrays," *IEEE Antennas Wireless Propag. Lett.*, vol. 11, pp. 101-104, 2012.

[40] F. Viani, F. Robol, M. Salucci, and R. Azaro, "Automatic EMI filter design through particle swarm optimization," *IEEE Trans. Electromagnet. Compat.*, vol. 59, no. 4, pp. 1079-1094, Aug. 2017.

[41] G. Oliveri, M. Salucci, and A. Massa, "Towards reflectarray digital twins - An EM-driven machine learning perspective," *IEEE Transactions on Antennas and Propagation - Special Issue on 'Machine Learning in Antenna Design, Modeling, and Measurements,'* vol. 70, no. 7, pp. 5078-5093, July 2022.

[42] M. Salucci, L. Tenuti, G. Oliveri, and A. Massa, "Efficient prediction of the EM response of reflectarray antenna elements by an advanced statistical learning method," *IEEE Trans. Antennas Propag.*, vol. 66, no. 8, pp. 3995-4007, Aug. 2018.